



Katarzyna Grebieszko
Warsaw University of Technology



for the NA49 and NA61 Collaborations

Search for the QCD critical point at SPS energies

EPS HEP 2009
Krakow, Poland
July 16th - 22th, 2009

CERN (Super Proton Synchrotron and Large Hadron Collider accelerators)



Circumference of the SPS tunnel – 6 km
Circumference of the LHC tunnel – 27 km

Some theoretical (lattice) calculations locate the **critical point (CP) of strongly interacting matter** in the SPS energy range

$$(T^{\text{CP}}, \mu_B^{\text{CP}}) = (162 \pm 2, 360 \pm 40) \text{ MeV}$$

Fodor, Katz, JHEP **0404**, 050 (2004)

$$(T^{\text{CP}}/T_c, \mu_B^{\text{CP}}/T^{\text{CP}}) = (\approx 0.95, 1.1 \pm 0.2)$$

T_c – cross-over temperature at $\mu_B = 0$

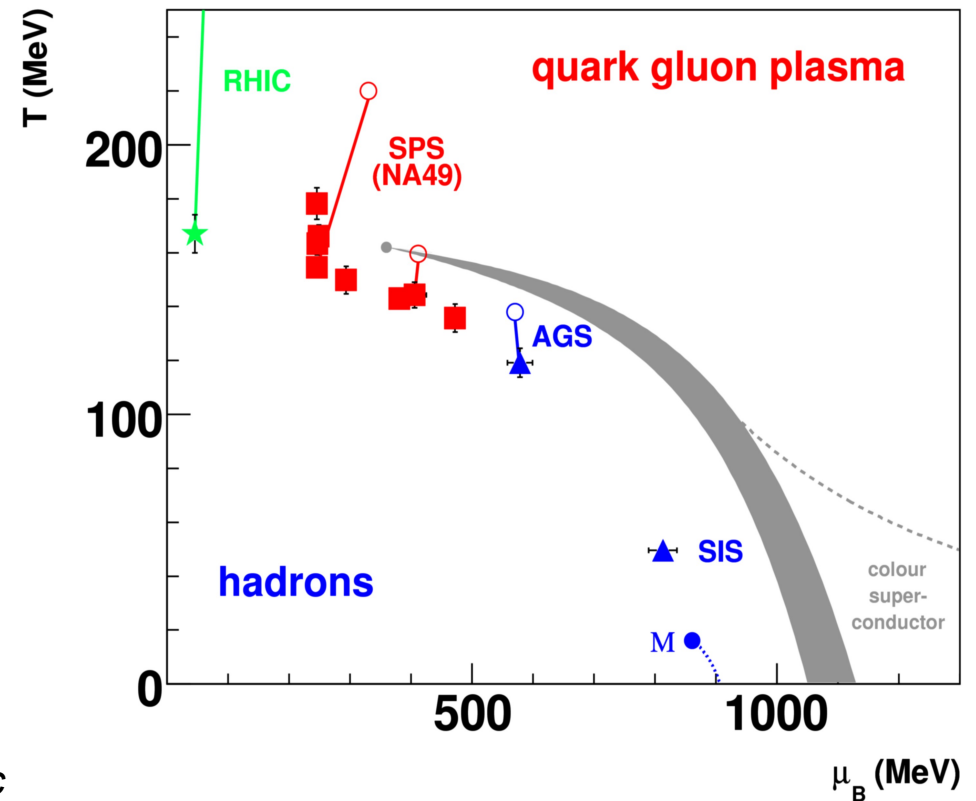
Gavai, Gupta, PRD**71**, 114014 (2005)

Critical opalescence is observed in most liquids (including water)

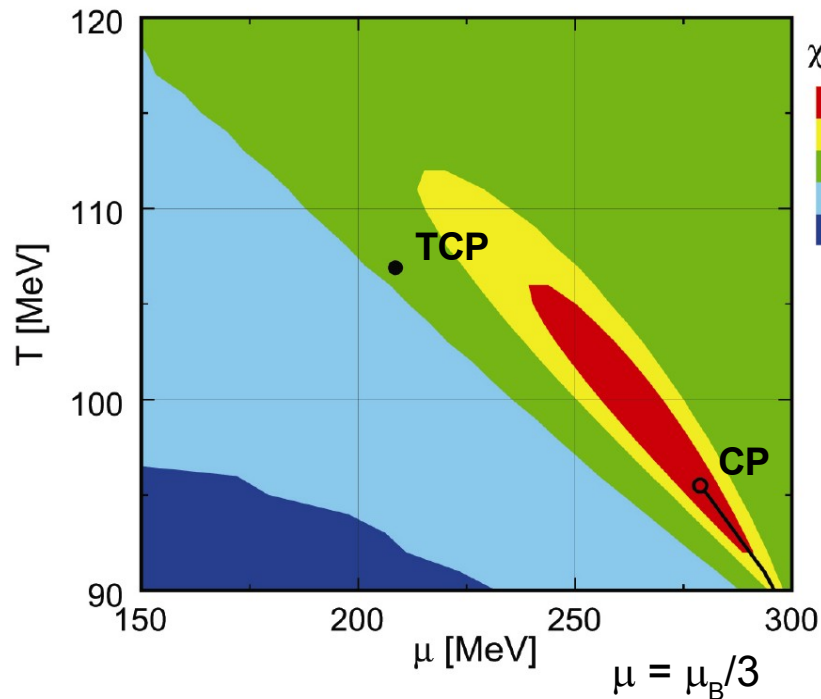
“As the fluid cools down under conditions such that it passes near the end point of the boiling transition, it goes from transparent to opalescent to transparent as the end point is approached and then passed. This non-monotonic phenomenon is due to scattering of light on critical long wavelength density fluctuations (...)” Stephanov, Rajagopal, Shuryak, PRD**60**, 114028 (1999)

For strongly interacting matter
maximum of CP signal expected when
freeze-out happens near CP

very interesting region covered by NA49 !

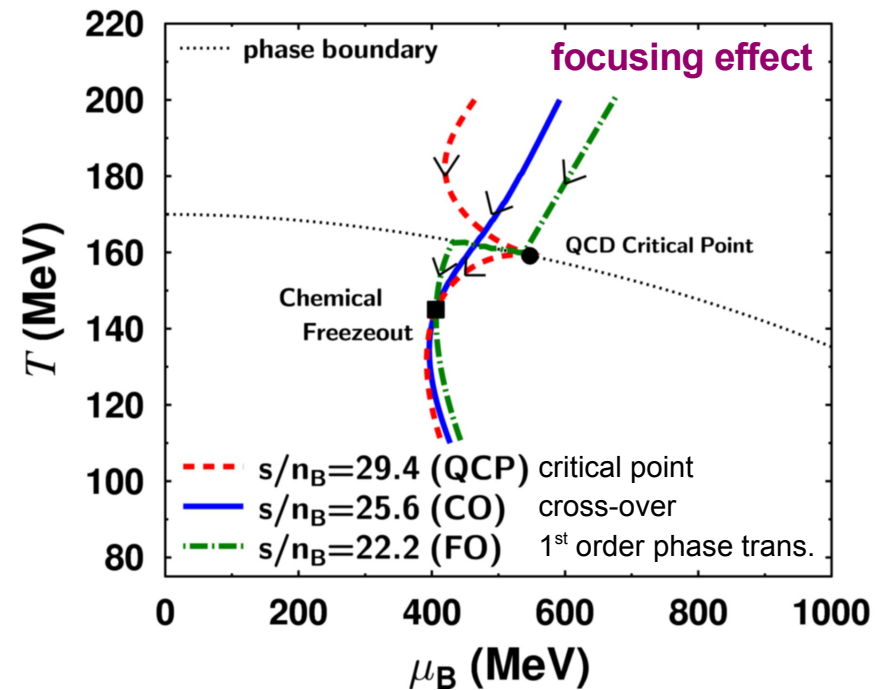


CP should be searched above the energy of the onset of deconfinement.
From NA49 data $E_{\text{OD}} \cong 30A \text{ GeV}$
(C. Alt et al., PRC**77**, 024903 (2008))



Hatta, Ikeda PRD**67**, 014028 (2003)

Effect of critical point extends over a critical region with $\sigma(\mu_B)$ and $\sigma(T)$



For a given chemical freeze-out point three isentropic trajectories ($n_B/s = \text{const.}$) are shown

Askawa et al. PRL**101**, 122302 (2008)

The presence of the critical point can deform the trajectories describing the evolution of the expanding fireball in the (T, μ_B) phase diagram

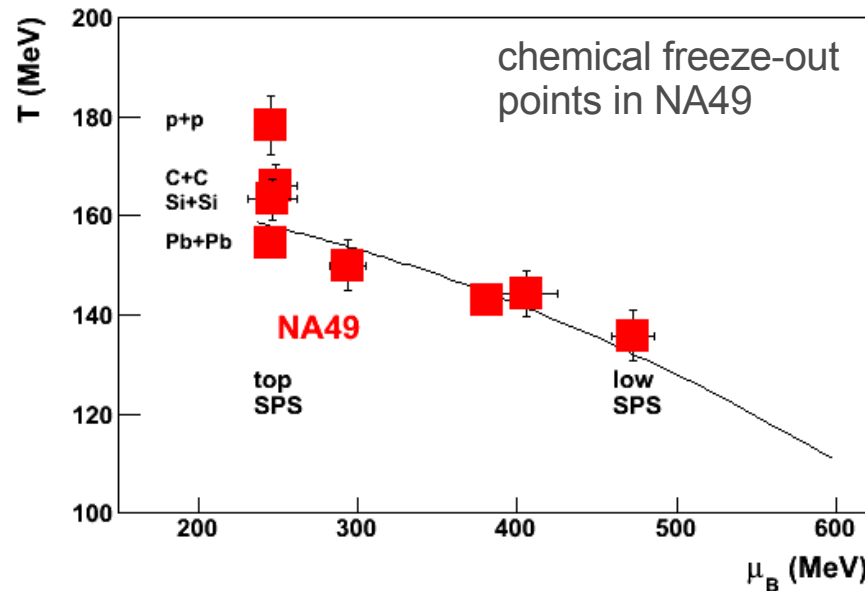
⇒ We do not need to hit precisely the critical point because **a large region can be affected!**

At CP enlarged fluctuations of multiplicity and mean transverse momentum

Stephanov, Rajagopal, Shuryak, PRD**60**, 114028 (1999)

Other signatures of CP also proposed: **transverse mass spectra of baryons and anti-baryons, (elliptic flow of baryons and mesons and intermittency in transverse momentum space of di-pions** not discussed here)

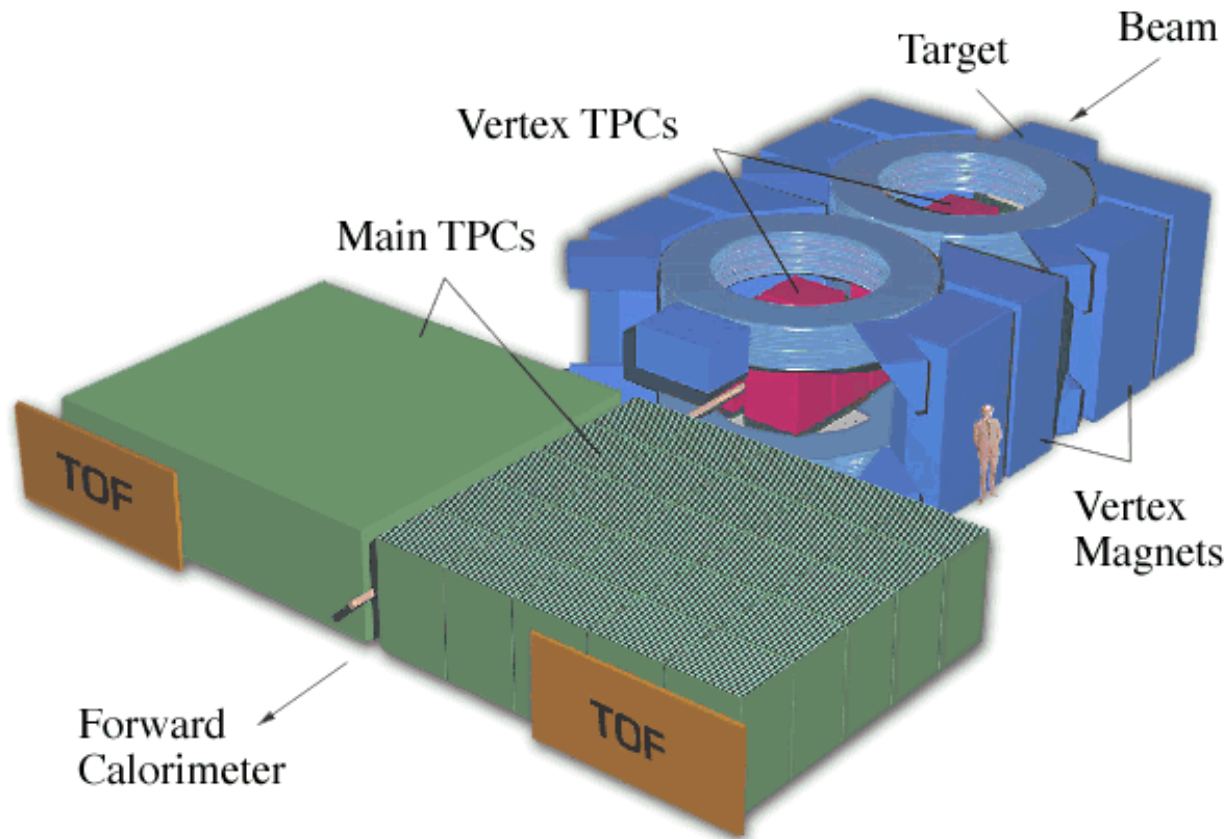
(T, μ_B) phase diagram can be scanned by varying energy and system size



Strategy to look for critical point in NA49:

- Energy scan (beam 20A-158A GeV) with central Pb+Pb collisions
- System size dependence (different ions) at 158A GeV (top SPS energy)

NA49 (fixed target) experiment at CERN SPS



Operating since 1994; p+p, C+C, Si+Si and Pb+Pb interactions at center of mass energy
6.3 – 17.3 GeV for N+N pair

Hadron spectrometer

Four TPCs; two VTTPCs (1/2) in the **B** field and two others MTTPCs (R/L) outside;
for a precise measurement of **p** and dE/dx

Large acceptance: $\approx 50\%$

High momentum resolution:

$$\sigma(p)/p^2 \approx 10^{-4} \quad ((GeV/c)^{-1})$$

Good particle identification:

$$\begin{aligned} \sigma(TOF) &\approx 60 \text{ ps}, \\ \sigma(dE/dx)/\langle dE/dx \rangle &\approx 0.04, \\ \sigma(m_{inv}) &\approx 5 \text{ MeV} \end{aligned}$$

Centrality determination:

Forward Calorimeter
(energy of projectile spectators)

Event-by-event transverse momentum and multiplicity fluctuations

Φ_{p_T} - measures transverse momentum fluctuations on event-by-event basis

single-particle variable $z_{p_T} = p_T - \bar{p}_T$

\bar{p}_T - inclusive average

event variable $Z_{p_T} = \sum_{i=1}^N (p_{T_i} - \bar{p}_T)$

(summation runs over particles in a given event)

$$\Phi_{p_T} = \sqrt{\frac{\langle Z_{p_T}^2 \rangle}{\langle N \rangle}} - \sqrt{z_{p_T}^2}$$

$\langle \dots \rangle$ - averaging over events

ω - measures multiplicity fluctuations on event-by-event basis

Scaled variance of multiplicity distribution

$$\omega = \frac{V(N)}{\langle N \rangle}$$

where variance $V(N) = \langle N^2 \rangle - \langle N \rangle^2$

If A+A is a **superposition** of independent N+N

$$\Phi_{p_T}(A+A) = \Phi_{p_T}(N+N)$$

Φ_{p_T} is independent of N_{part} fluctuations

$$\omega(A+A) = \omega(N+N) + \langle n \rangle \omega_{part}$$

$\langle n \rangle$ - mean multiplicity of hadrons from a single N+N

ω_{part} - fluctuations in N_{part}

ω is strongly dependent on N_{part} fluctuations

For a system of **independently emitted particles** (no inter-particle correlations)

$$\Phi_{p_T} = 0$$

For **Poissonian multiplicity distribution**

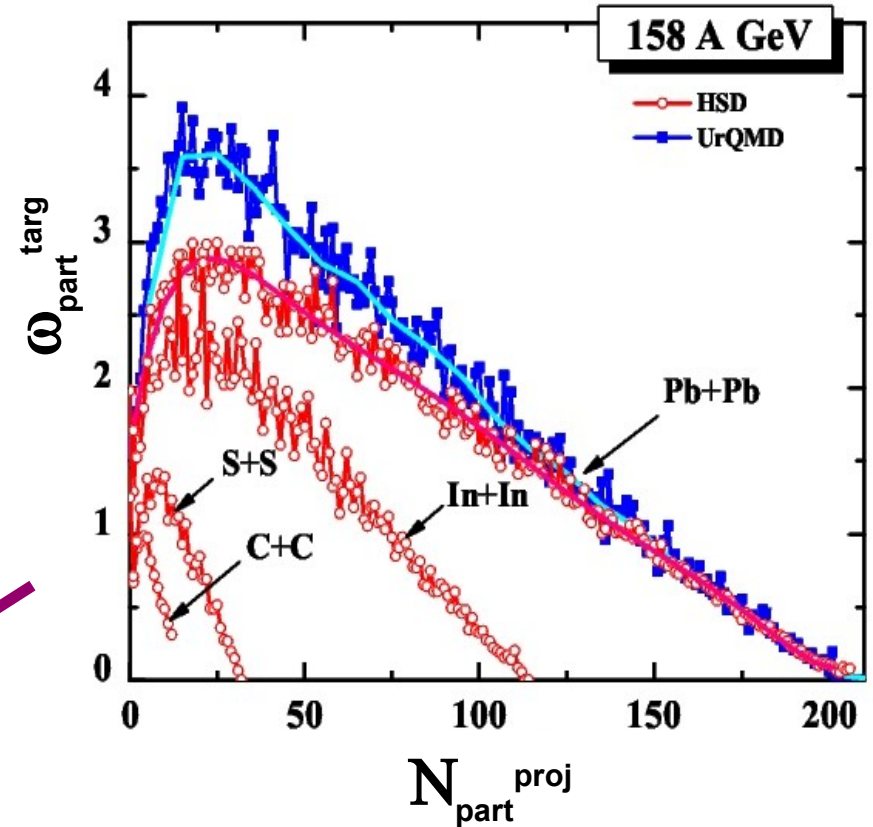
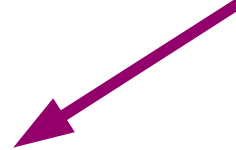
$$\omega = 1$$

In NA49 fixed target experiment

- $N_{\text{part}}^{\text{proj}}$ can be fixed (spectator energy measured by Forward Calorimeter)
- $N_{\text{part}}^{\text{targ}}$ cannot be measured and its fluctuations can be suppressed only by selection of very central collisions



Multiplicity fluctuations (ω) presented here are for very central (1%) collisions



$\omega_{\text{part}}^{\text{targ}}$ - fluctuations in the number of target participants for a fixed $N_{\text{part}}^{\text{proj}}$

Konchakovski et al., PRC**73**, 034902 (2006),
and private communication

Data sets and kinematic cuts (for Φ_{pT} and ω measurements):

- p+p, central and semi-central A+A collisions: 1% most centr. for ω and 5-15% for Φ_{pT}
- **forward-rapidity region**
- limited azimuthal acceptance (for details see corresponding papers)

Critical point predictions for multiplicity and transverse moment. fluctuations

Magnitude of fluctuations at CP from Stephanov, Rajagopal, Shuryak PRD**60**, 114028 (1999)

with correlation length $\xi = \min (c_1 A^{1/3}, c_2 A^{1/9}) =$

$\min (\text{limit due to finite system size, limit due to finite life time})$

(M. Stephanov, private communication)

where c_1 and c_2 are fixed such that

- $\xi(\text{Pb+Pb}) = 6 \text{ fm}$ and $\xi(\text{p+p}) = 2 \text{ fm}$ ($c_1 = 2, c_2 = 3.32$)
- $\xi(\text{Pb+Pb}) = 3 \text{ fm}$ and $\xi(\text{p+p}) = 1 \text{ fm}$ ($c_1 = 1, c_2 = 1.66$)

Width of CP region in (T, μ_B) plane based on Hatta, Ikeda PRD**67**, 014028 (2003)

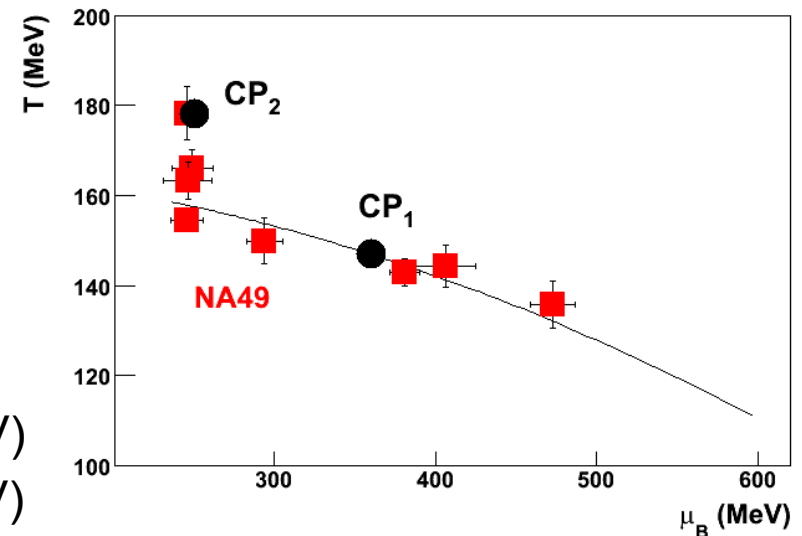
$\sigma(\mu_B) \approx 30 \text{ MeV}$ and $\sigma(T) \approx 10 \text{ MeV}$

Chemical freeze-out parameters, $T(A, \sqrt{s_{NN}})$ and $\mu_B(A, \sqrt{s_{NN}})$ from Beccatini, Manninen, Gaździcki PRC**73**, 044905 (2006)

Location of the Critical Point:

two examples considered

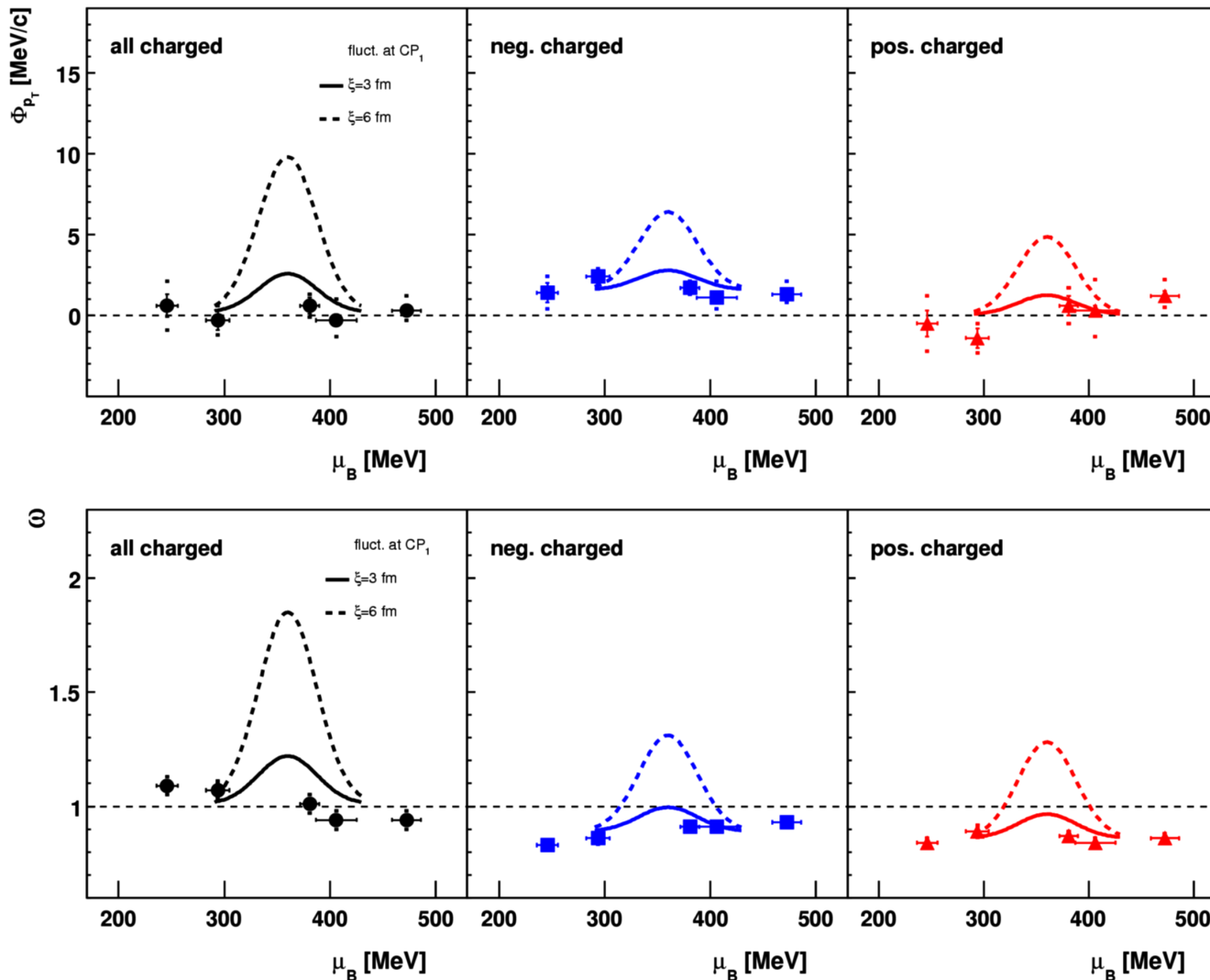
- $\mu_B(\text{CP}_1) = 360 \text{ MeV}$ (Fodor, Katz JHEP **0404**, 050 (2004))
 $T(\text{CP}_1) \approx 147$ (chemical freeze-out temperature T_{chem} for central Pb+Pb at $\mu_B = 360 \text{ MeV}$)
- $\mu_B(\text{CP}_2) \cong 250 \text{ MeV}$ (μ_B for A+A collisions at 158A GeV)
 $T(\text{CP}_2) = 178 \text{ MeV}$ (T_{chem} for p+p collisions at 158 GeV)



Energy dependence for central Pb+Pb

→ Average p_T fluctuations (PRC79, 044904 (2009))

→ Multiplicity fluctuations (PRC78, 034914 (2008))



CP_1 location:

$$\mu_B(CP_1) = 360 \text{ MeV}$$

$T(CP_1) \approx 147$ (chemical freeze-out temperature for Pb+Pb at $\mu_B = 360$ MeV)

base-lines for CP_1 predictions (curves) are mean Φ_{pT} and ω values for 5 energies

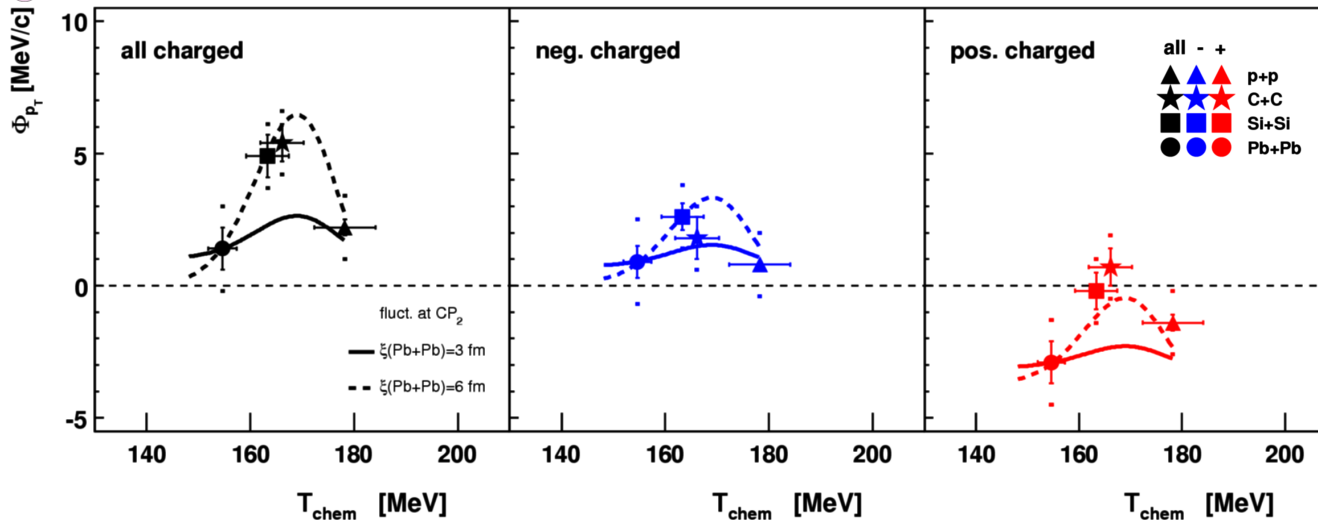
Data do not provide evidence for critical point fluctuations

→ No significant energy dependence at SPS energies

System size dependence at 158A GeV

→ Average p_T fluctuations (PRC70, 034902, 2004))

→ Multiplicity fluctuations (pp: PRC75, 064904 (2007); PbPb: PRC78, 034914 (2008); CC, SiSi: B. Lungwitz, PhD)



CP_2 location:

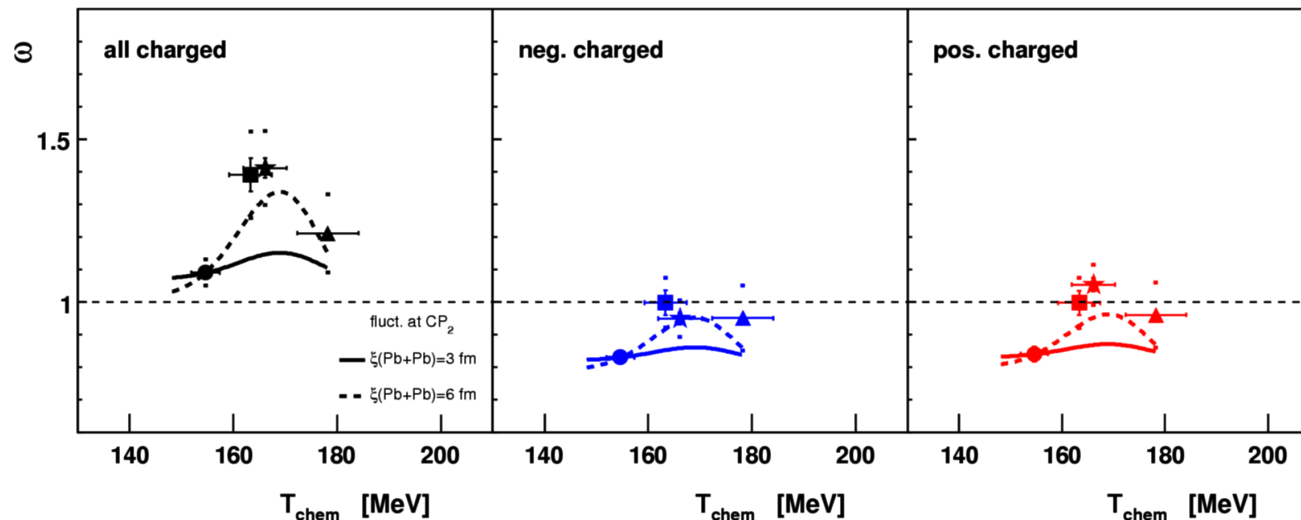
$$\mu_B(CP_2) \cong 250 \text{ MeV} = \mu_B(A+A \text{ at } 158A \text{ GeV})$$

$$T(CP_2) = 178 \text{ MeV} = T_{\text{chem}}(p+p)$$

CP_2 predictions (curves)

normalized to reproduce Φ_{pT}

and ω value for central Pb+Pb collisions



Data are consistent with the CP_2 predictions

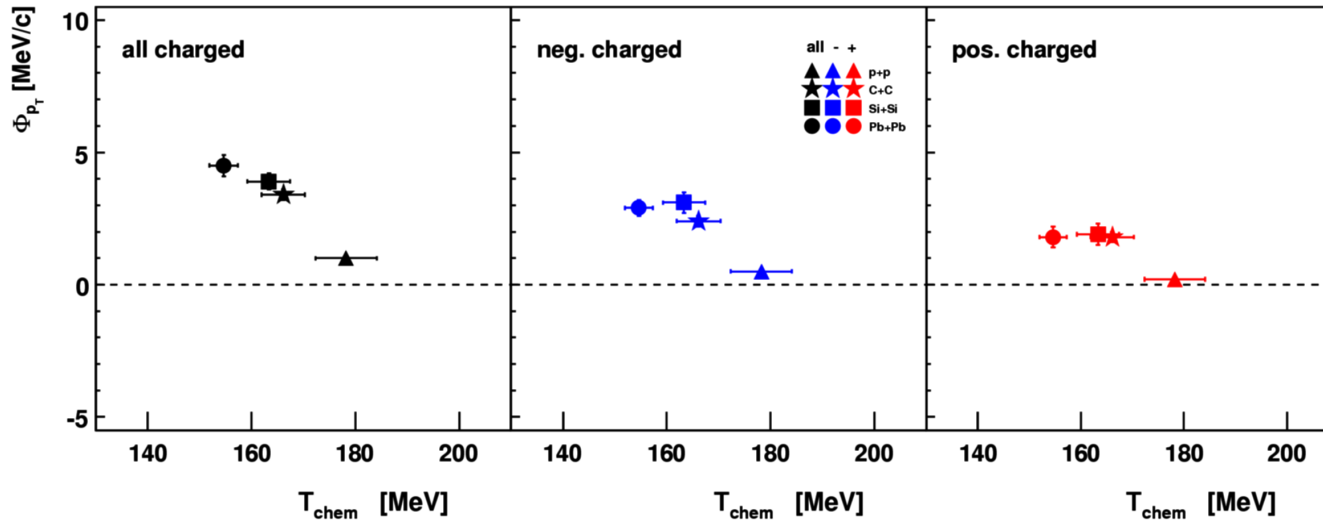
→ Maximum of Φ_{pT} and ω observed for C+C and Si+Si

→ Increase ~ two times larger for all charged than for negatively charged particles

Expectations: fluctuations due to the critical point originate mainly from low p_T pions

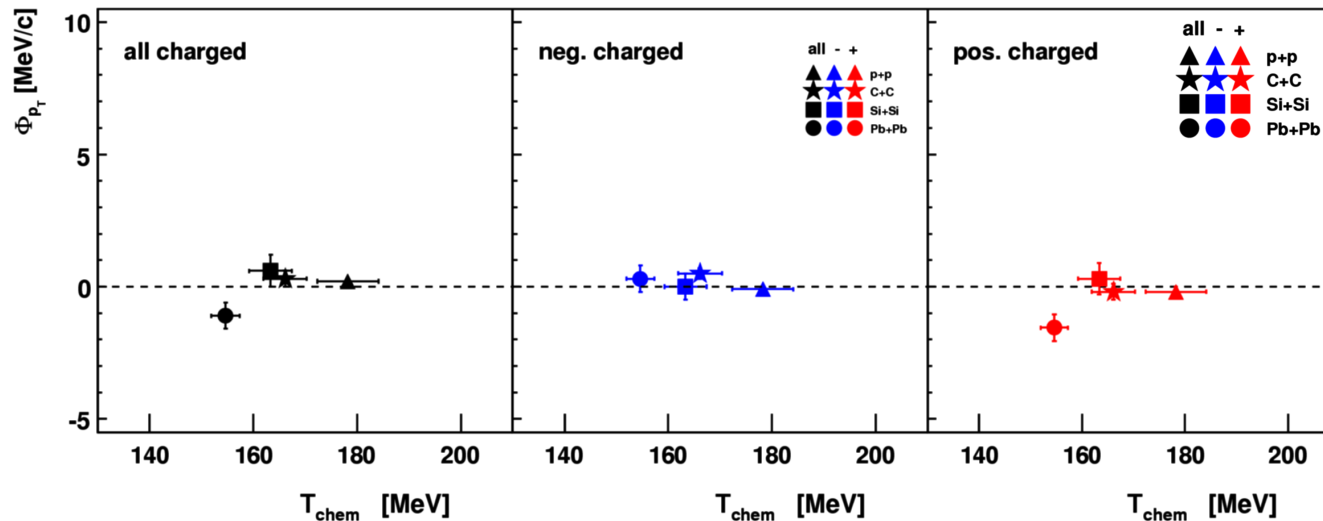
Stephanov, Rajagopal, Shuryak, PRD60, 114028 (1999)

NA49 results for low and high p_T regions:



low p_T region
 $p_T < 0.5$ GeV/c
signal observed

NA49 preliminary



high p_T region
 $p_T > 0.5$ GeV/c
**fluctuations
 consistent with
 zero**

→ **Correlations observed predominantly at low p_T**

→ **No more maximum of Φ_{pT} due to large correlations in Pb+Pb; their origin currently analyzed** (short range correlations considered)

Transverse mass spectra of baryons and anti-baryons

The presence of a critical point can deform the trajectories describing the evolution of the expanding fireball in the $(T - \mu_B)$ phase diagram. The critical point serves as an attractor of the hydrodynamical trajectories. Askawa et. al. PRL**101**, 122302 (2008):

If the average emission time of hadrons is a function of transverse velocity (β_T) **this deformation will change the β_T dependence of \bar{p}/p ratio** provided that the fireball passes **in the vicinity of the critical point**

Expected observable: the **\bar{p}/p ratio should fall with increasing transverse momentum** instead of a rise (\bar{p} annihilation) or flat behavior in a scenario without the critical point

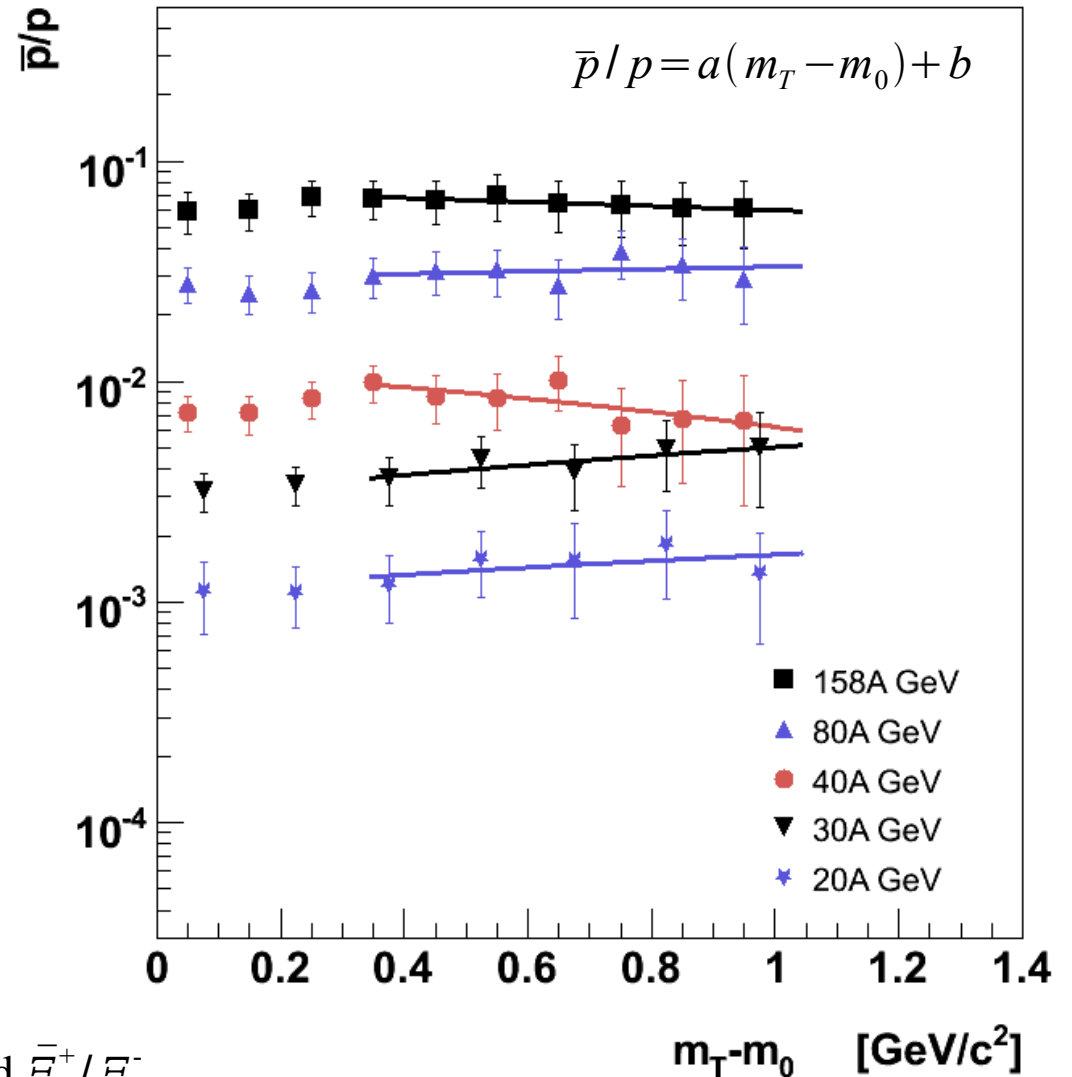
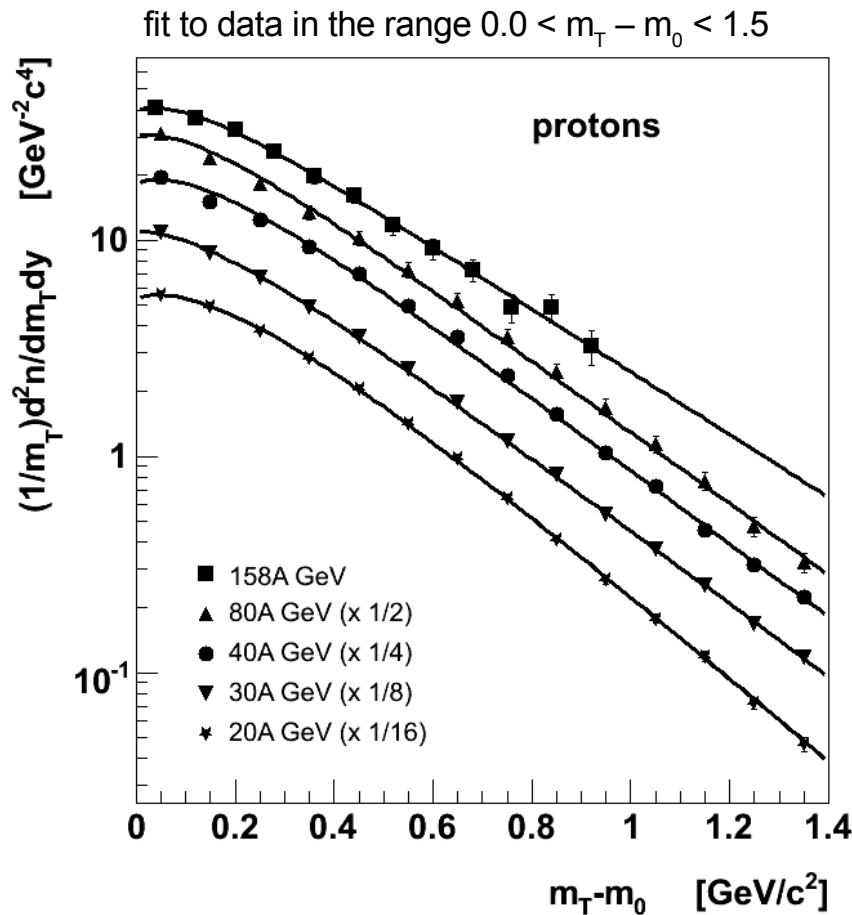
(For UrQMD+THERMINATOR predictions see also Luo et al. arXiv:0903.0024)

Energy dependence for central Pb+Pb

→ \bar{p}/p ratio versus m_T (PRC73, 044910 (2006))

$$\frac{1}{m_T} \frac{d^2 n}{dm_T dy} = C_1 \exp(-(m_T - m_0)/T_{slope}) + C_2 \exp(-(m_T - m_0)/T')$$

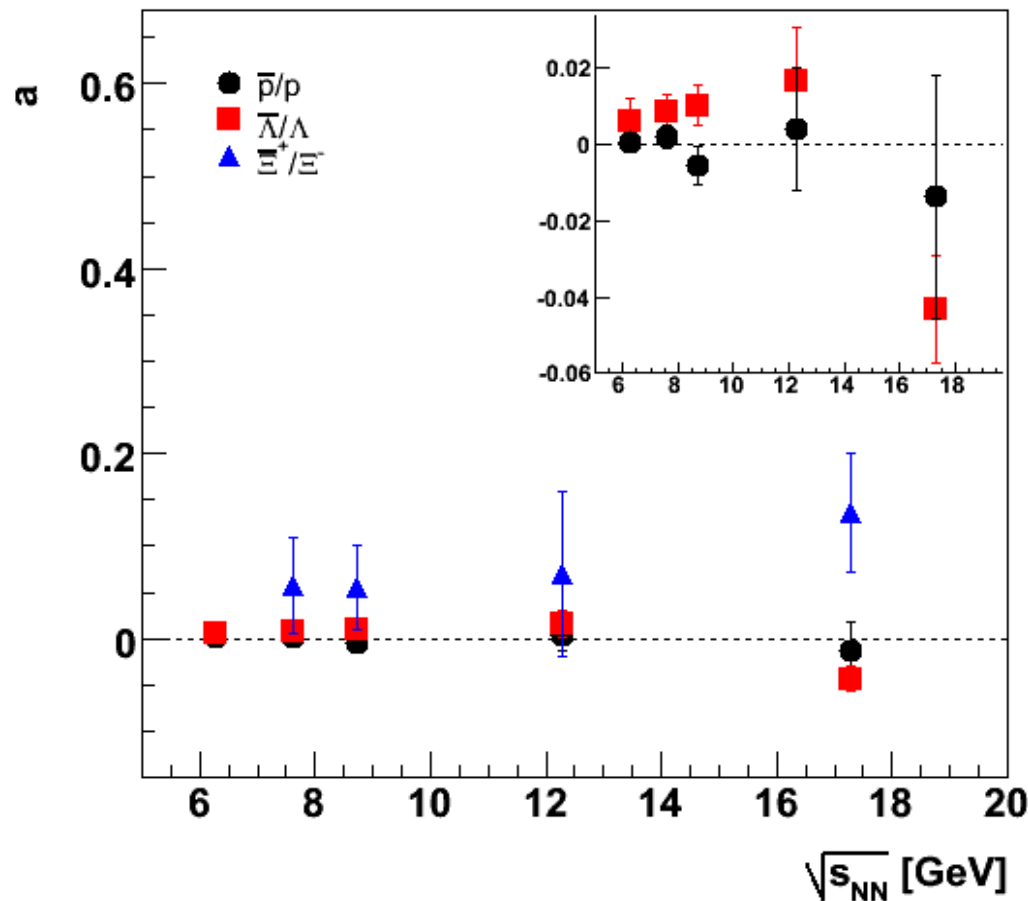
Points for \bar{p} divided by fitted curves (left) for protons



Similar procedure applied also for $\bar{\Lambda}/\Lambda$ and \bar{E}^+/E^-
PRC73, 044910 (2006); PRC78, 034918 (2008)

Energy dependence for central Pb+Pb → Anti-baryon/baryon ratio versus m_T

$$\text{anti-baryon/baryon} = a (m_T - m_0) + b$$



→ No significant energy dependence of slope parameter (a) in anti-baryon to baryon ratio.

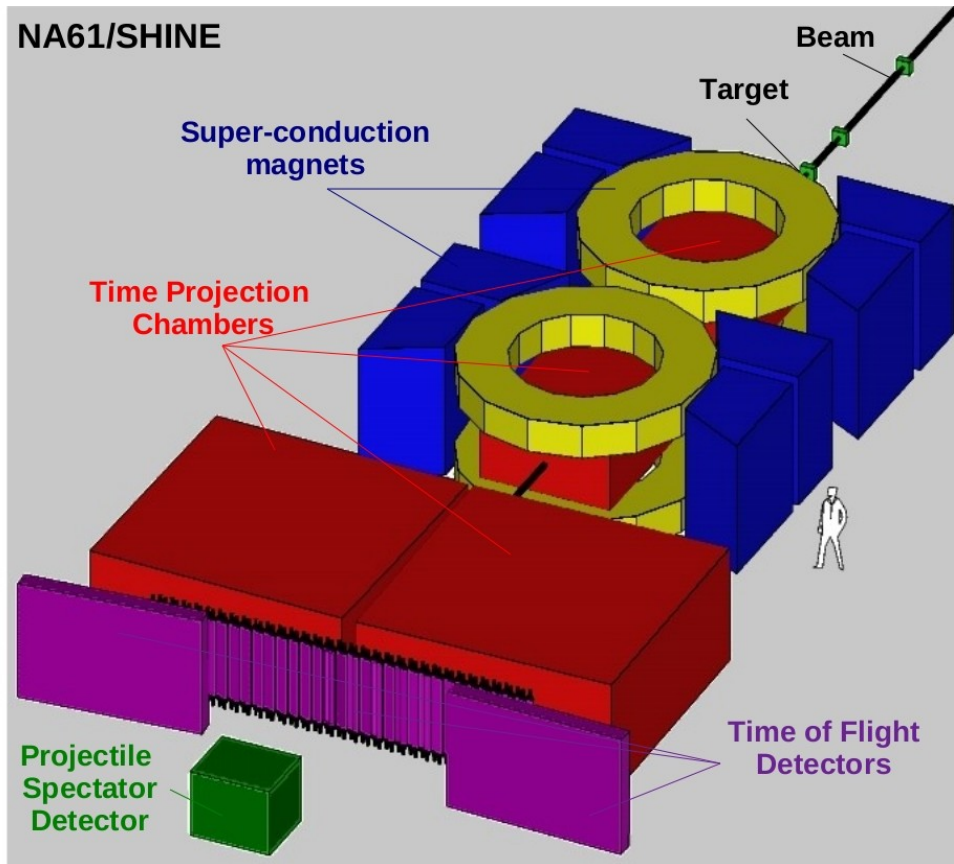
No evidence for the critical point

Summary of NA49 results

- Results on hadron production in A+A collisions at the CERN SPS energies related to the search for the critical point of strongly interacting matter have been presented
- **There are no indications of the critical point in the energy dependence** of multiplicity and mean transverse momentum fluctuations, and ratios of the anti-baryon/baryon transverse mass spectra **in central Pb+Pb collisions**
- **The system size dependence at 158A GeV shows:**
 - a **maximum of mean p_T and multiplicity fluctuations** in the complete p_T range → **consistent with CP_2 predictions**
 - an **increase** (from p+p up to Pb+Pb) **of mean p_T fluctuations in the low p_T region (reason currently under study)**; high p_T particles show no fluctuation signal
- The low p_T region will be carefully analyzed for the effects of short range correlations on Φ_{p_T} and ω
- A detailed energy and system-size scan is necessary to establish the existence of the critical point → NA61/SHINE

Search for the critical point in NA61/SHINE

SHINE (fixed target) experiment at CERN SPS

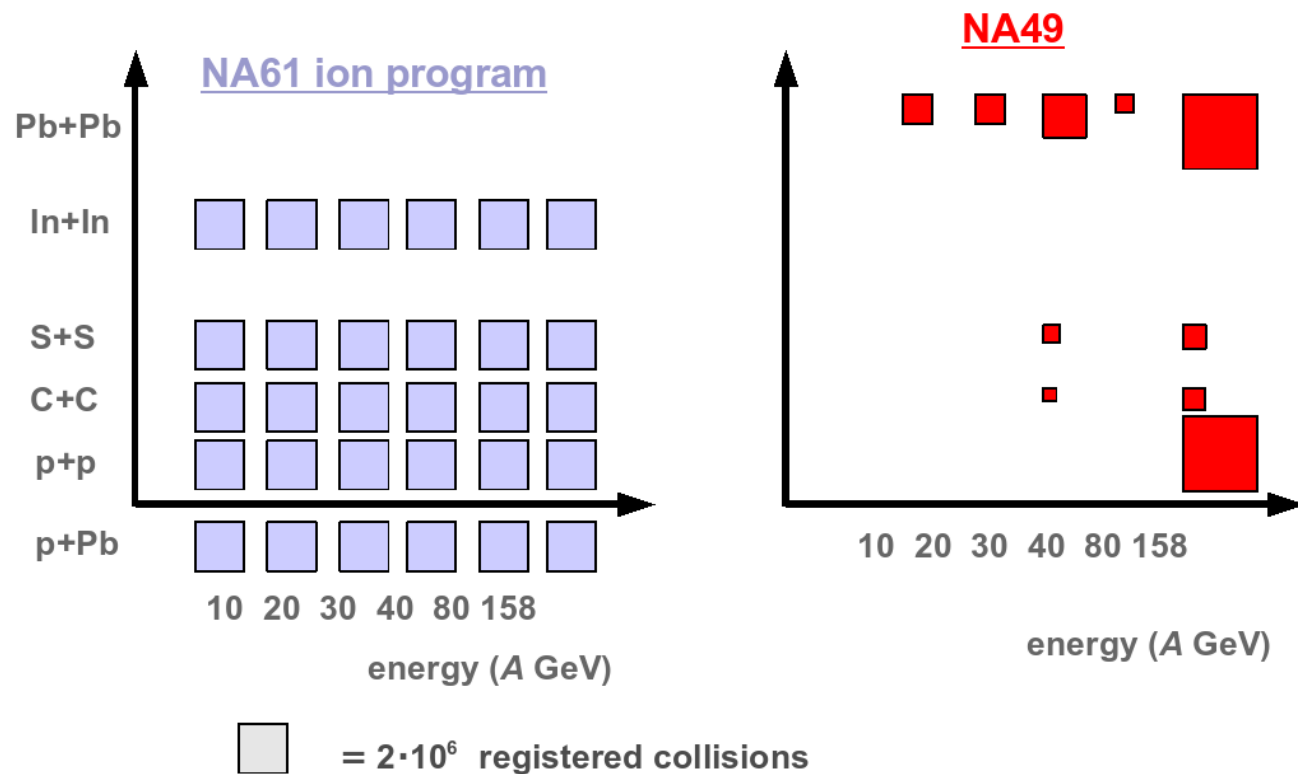


NA61/SHINE physics program:

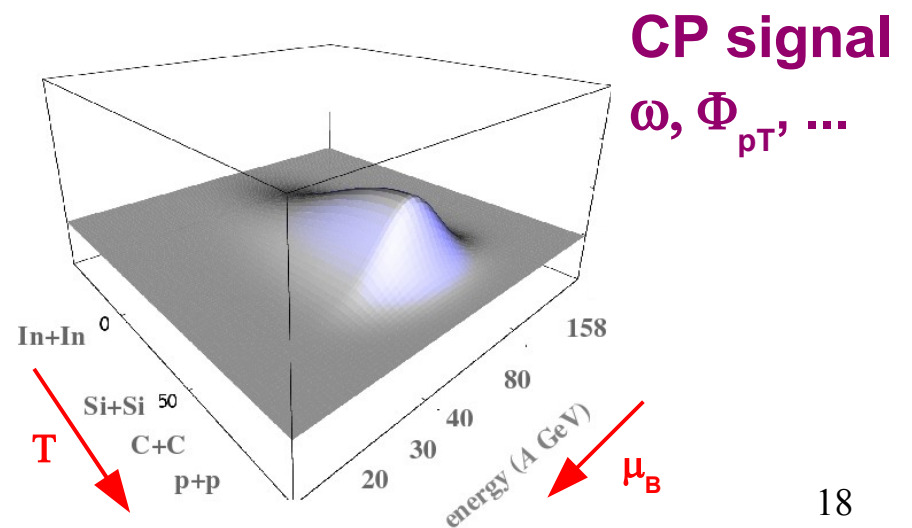
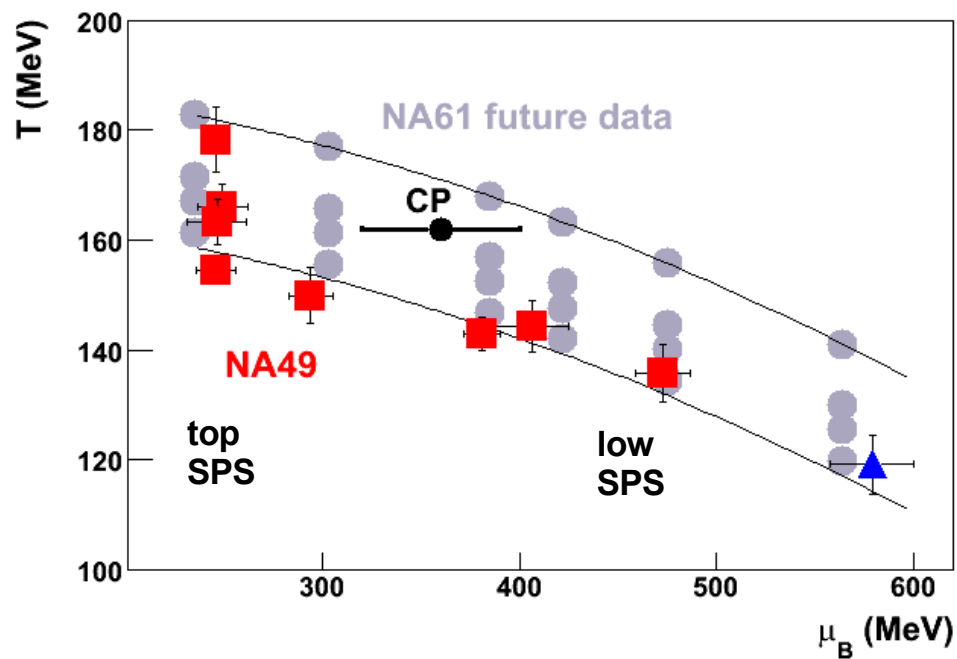
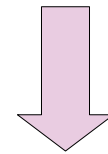
- **Critical Point and Onset of Deconfinement,**
- High p_T physics
- Neutrino physics
- Cosmic-ray physics

Main upgrades:

- 2007: Construction of the **forward ToF wall**
- 2008: Replacement of the TPC digital **read-out** and **DAQ** (increase of the event rate by a factor of ≈ 10)
- Planned: Replacement of Forward Calorimeter (VETO) by **Projectile Spectator Detector**



Non-monotonic dependence of critical point signal on control parameters (energy, centrality, ion size) can help to locate the critical point



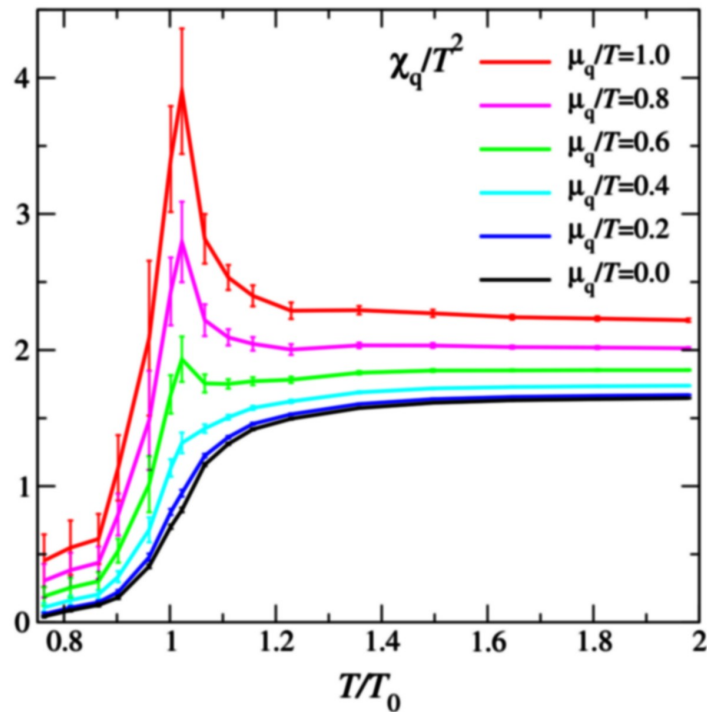
NA49 Collaboration:

T. Anticic, B. Baatar, D. Barna, J. Bartke, L. Betev, H. Białkowska, C. Blume, B. Boimska, M. Botje, J. Bracinik, P. Buncic, V. Cerny, P. Christakoglou, P. Chung, O. Chvala, J. G. Cramer, P. Csato, P. Dinkelaker, V. Eckardt, Z. Fodor, P. Foka, V. Friese, J. Gal, M. Gaździcki, V. Genchev, E. Gładysz, K. Grebieszko, S. Hegyi, C. Hohne, K. Kadija, A. Karev, D. Kikola, V. I. Kolesnikov, E. Kornas, R. Korus, M. Kowalski, M. Kreps, D. Kresan, A. Laszlo, R. Lacey, M. van Leeuwen, P. Levai, L. Litov, B. Lungwitz, M. Makariev, A. I. Malakhov, M. Mateev, G. L. Melkumov, A. Mischke, M. Mitrovski, J. Molnar, St. Mrówczyński, V. Nikolic, G. Palla, A. D. Panagiotou, D. Panayotov, A. Petridis, W. Peryt, M. Pikna, J. Pluta, D. Prindle, F. Puhlhofer, R. Renfordt, C. Roland, G. Roland, M. Rybczyński, A. Rybicki, A. Sandoval, N. Schmitz, T. Schuster, P. Seyboth, F. Sikler, B. Sitar, E. Skrzypczak, M. Slodkowski, G. Stefanek, R. Stock, C. Strabel, H. Strobele, T. Susa, I. Szentpetery, J. Sziklai, M. Szuba, P. Szymanski, V. Trubnikov, M. Utvic, D. Varga, M. Vassiliou, G. I. Veres, G. Vesztergombi, D. Vranic, Z. Włodarczyk, A. Wojtaszek-Szwarc, I. K. Yoo

NA61/SHINE Collaboration:

N. Abgrall, A. Aduszkiewicz, B. Andrieu, T. Anticic, N. Antoniou, A. G. Asryan, B. Baatar, A. Blondel, J. Blumer, L. Boldizsar, A. Bravar, J. Brzychczyk, S. A. Bunyatov, K.-U. Choi, P. Christakoglou, P. Chung, J. Cleymans, D. A. Derkach, F. Diakonov, W. Dominik, J. Dumarchez, R. Engel, A. Ereditato, G. A. Feofilov, Z. Fodor, M. Gaździcki, M. Golubeva, K. Grebieszko, F. Guber, T. Hasegawa, A. Haungs, M. Hess, S. Igoikin, A. S. Ivanov, A. Ivashkin, K. Kadja, N. Katrynska, D. Kielczewska, D. Kikoła, J.-H. Kim, T. Kobayashi, V. I. Kolesnikov, D. Koley, R. S. Koleyatov, V. P. Kondratiev, A. Kurepin, R. Lacey, A. Laszlo, S. Lehmann, B. Lungwitz, V. V. Lyubushkin, A. Maevskaya, Z. Majka, A. I. Malakhov, A. Marchionni, A. Marcinek, M. Di Marco, I. Maris, V. Matveev, G. L. Melkumov, A. Meregaglia, M. Messina, C. Meurer, P. Mijakowski, M. Mitrovski, T. Montaruli, St. Mrówczyński, S. Murphy, T. Nakadaira, P. A. Naumenko, V. Nikolic, K. Nishikawa, T. Palczewski, G. Palla, A. D. Panagiotou, W. Peryt, A. Petridis, R. Planeta, J. Pluta, B. A. Popov, M. Posiadała, P. Przewłocki, W. Rauch, M. Ravonel, R. Renfordt, D. Rohrich, E. Rondio, B. Rossi, M. Roth, A. Rubbia, M. Rybczyński, A. Sadovsky, K. Sakashita, T. Schuster, T. Sekiguchi, P. Seyboth, K. Shileev, A. N. Sissakian, E. Skrzypczak, M. Słodkowski, A. S. Sorin, P. Staszczel, G. Stefanek, J. Stepaniak, C. Strabel, H. Stroebele, T. Susa, I. Szentpetery, M. Szuba, A. Taranenko, R. Tsenov, R. Ulrich, M. Unger, M. Vassiliou, V. V. Vechernin, G. Vesztegombi, Z. Włodarczyk, A. Wojtaszek-Szwarc, J. G. Yi, I.-K. Yoo

back-up slides



For strongly interacting matter long range baryon density fluctuations expected

A picture supported by lattice calculations

Baryon density fluctuations appear to diverge for some critical value of the baryochemical potential

C. R. Allton, Phys. Rev. **D68** (2003), 014507

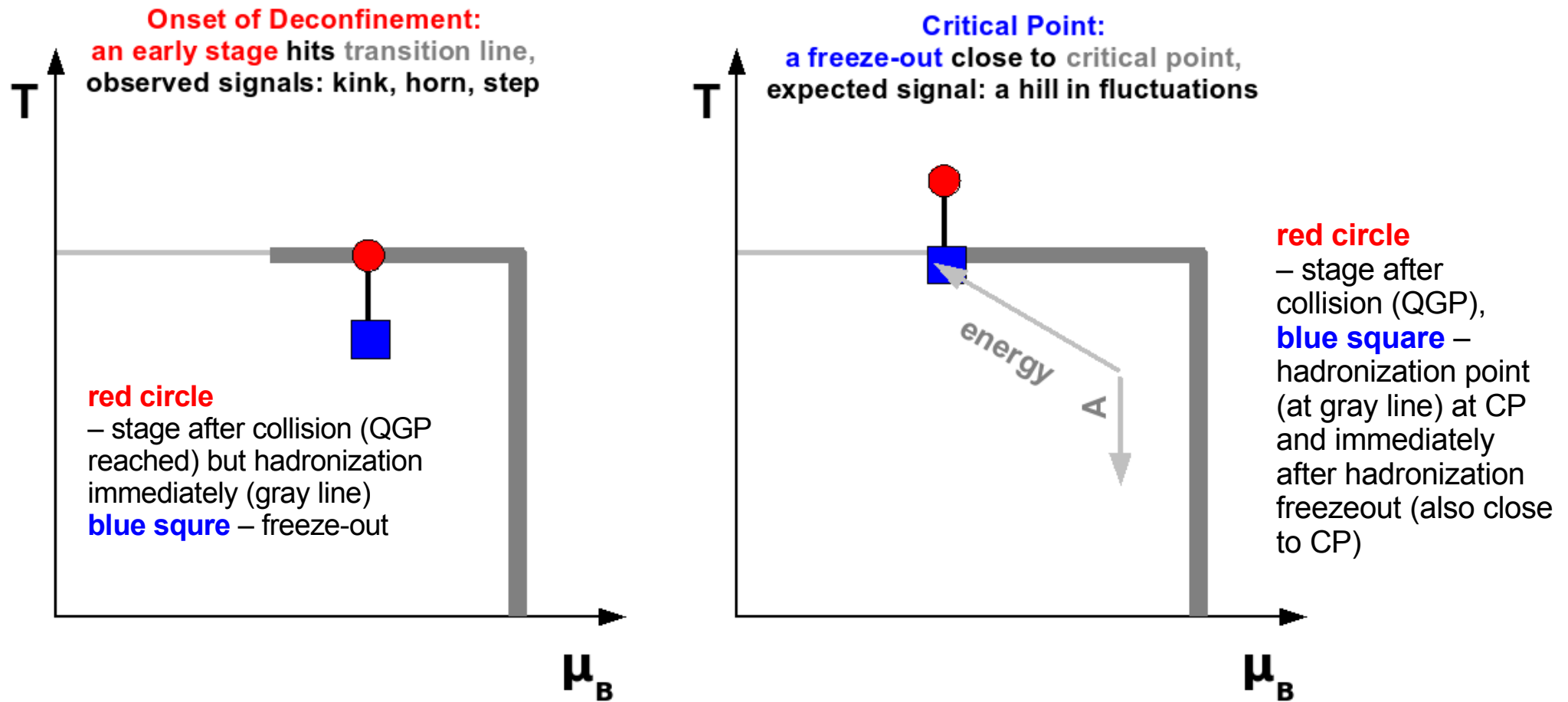
quark number susceptibility: $\chi_q \equiv \partial n_q / \partial \mu_q$,

T_0 – critical temperature for $\mu_q = 0$ ($\mu_B = 3\mu_q$)

CP should be searched above the phase transition energy as $E_{CP} > E_{OD}$

From NA49 data $E_{OD} \cong 30 A \text{ GeV}$

Reaching the phase transition (left) and hadronization and freeze-out at CP (right)



$$E(OoD) \approx 30A \text{ GeV} \leq E(OoC)$$

Data sets (for Φ_{pT} and ω measurements):

Energy dependence for central Pb+Pb collisions

- Central Pb+Pb interactions (7.2% most central for Φ_{pT} and 1% most central for ω)
- kinematic acceptance
 - for Φ_{pT} : forward-rapidity $1.1 < y_{\pi}^* < 2.6$ and $0.005 < p_T < 1.5$ GeV/c; $y_p^* < y_{beam}^* - 0.5$ (to reject projectile spectator domain)
 - for ω : forward rapidity region $1.1 < y_{\pi}^* < y_{beam}^*$
- limited azimuthal acceptance (for details see corresponding papers)

System size dependence at 158A GeV

- p+p, C+C (1%), Si+Si (1%) and Pb+Pb (1%) for ω ;
p+p, semi-central C+C (15.3%) and Si+Si (12.2%), 5% most central Pb+Pb for Φ_{pT}
- kinematic acceptance
 - for Φ_{pT} : forward-rapidity $1.1 < y_{\pi}^* < 2.6$ and $0.005 < p_T < 1.5$ GeV/c
 - for ω : forward rapidity region $1.1 < y_{\pi}^* < y_{beam}^*$ ($1.1 < y_{\pi}^* < 2.6$ for p+p points)
- limited azimuthal acceptance (for details see corresponding papers)

New (updated in 2008) predictions at CP (values for the energy scan):
Concerning Φ_{pT} (additive correction to uncorrelated particle production):

Remark: uncorrelated particle production results in $\Phi_{pT} = 0$

Assuming correlation length $\xi = 6$ fm

4π acceptance: 40 MeV/c (all charged)
20 MeV/c (one charge only)

acceptance correction in rapidity: 0.6

acceptance correction in azimuthal angle: 0.4 (common for all energies)

Finally for NA49 acceptance: $40 \cdot 0.6 \cdot 0.4 = 9.6$ MeV/c (all charged)
4.8 MeV/c (like-sign particles)

However, the correlation length may not exceed 3 fm...

Assuming correlation length $\xi = 3$ fm

4π acceptance: 10 MeV/c (all charged)
5 MeV/c (one charge only)

acceptance correction in rapidity: 0.6

acceptance correction in azimuthal angle: 0.4

Finally for NA49 acceptance: 2.4 MeV/c (all charged)
1.2 MeV/c (like-sign particles)

New (updated in 2008) **predictions at CP (values for the energy scan):**

Concerning ω (additive correction to uncorrelated particle production):

Remark: uncorrelated particle production results in $\omega = 1$

Assuming correlation length $\xi = 6$ fm

4π acceptance: 2 (all charged)

1 (one charge only)

acceptance correction in rapidity: 0.6

acceptance correction in azimuthal angle: 0.7 (depends on energy; here mean value for 5 energies)

Finally for NA49 acceptance: $2 \cdot 0.6 \cdot 0.7 = 0.84$ (all charged)

0.42 (like-sign particles)

Assuming correlation length $\xi = 3$ fm

4π acceptance: 0.5 (all charged)

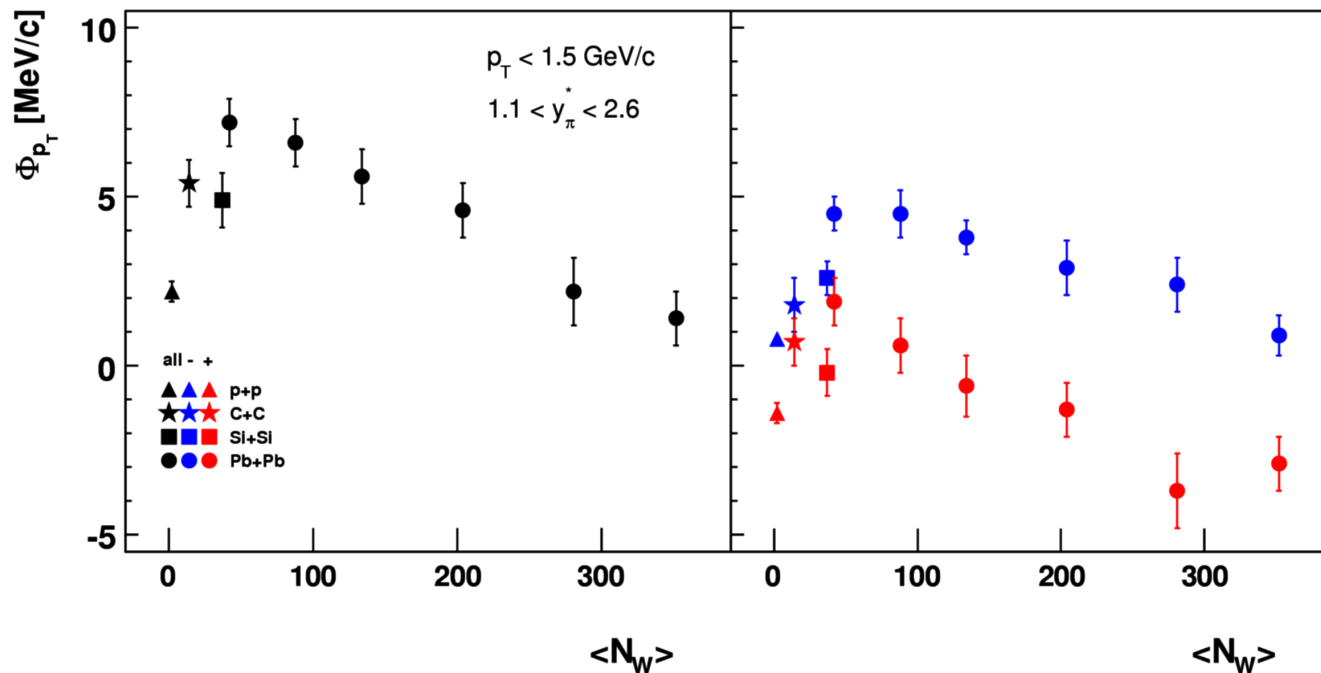
0.25 (one charge only)

acceptance correction in rapidity: 0.6

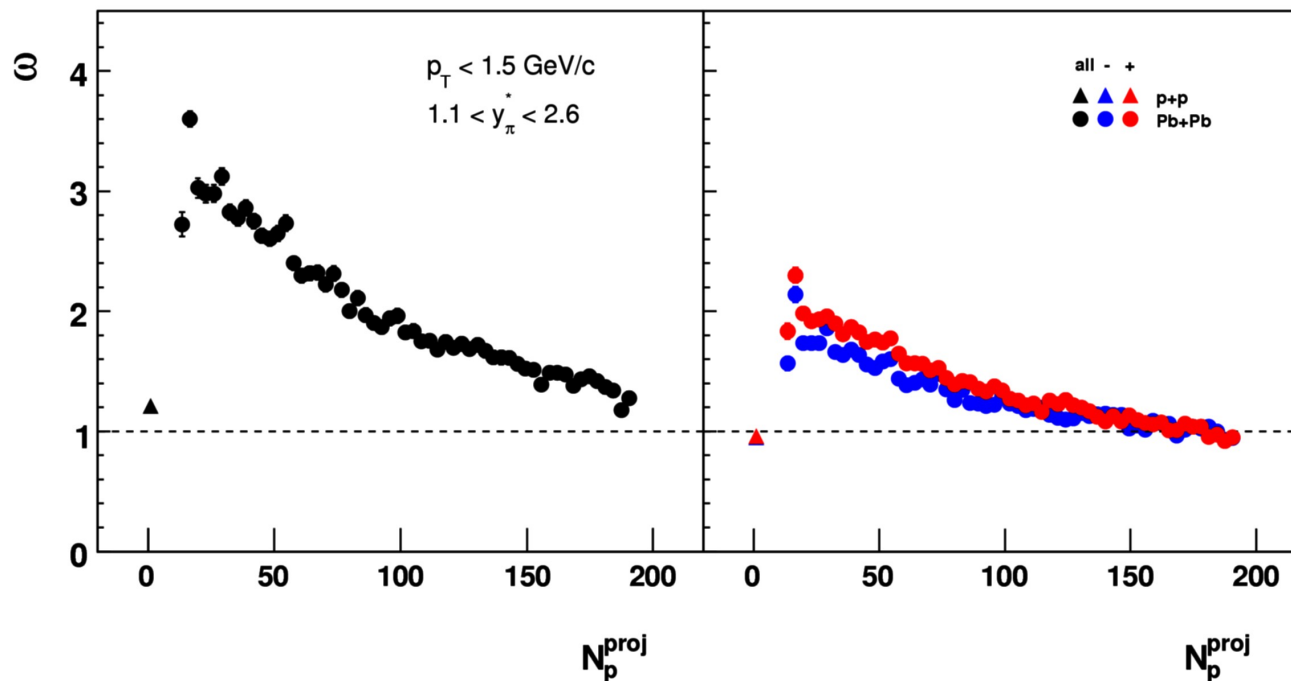
acceptance correction in azimuthal angle: 0.7

Finally for NA49 acceptance: 0.21 (all charged)

0.105 (like-sign particles)



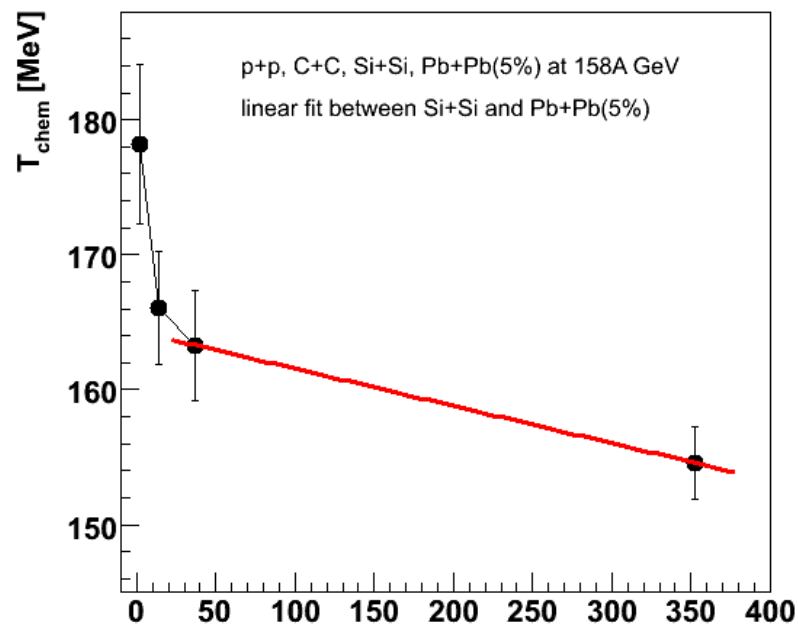
forward rapidity region
 $1.1 < y_\pi^* < 2.6$ and
 $0.005 < p_T < 1.5$ GeV/c
 limited azimuthal acceptance
 only statistical errors are shown



Very narrow bins in $N_{\text{part}}^{\text{proj}}$ but
 $N_{\text{part}}^{\text{target}}$ not measured in NA49.

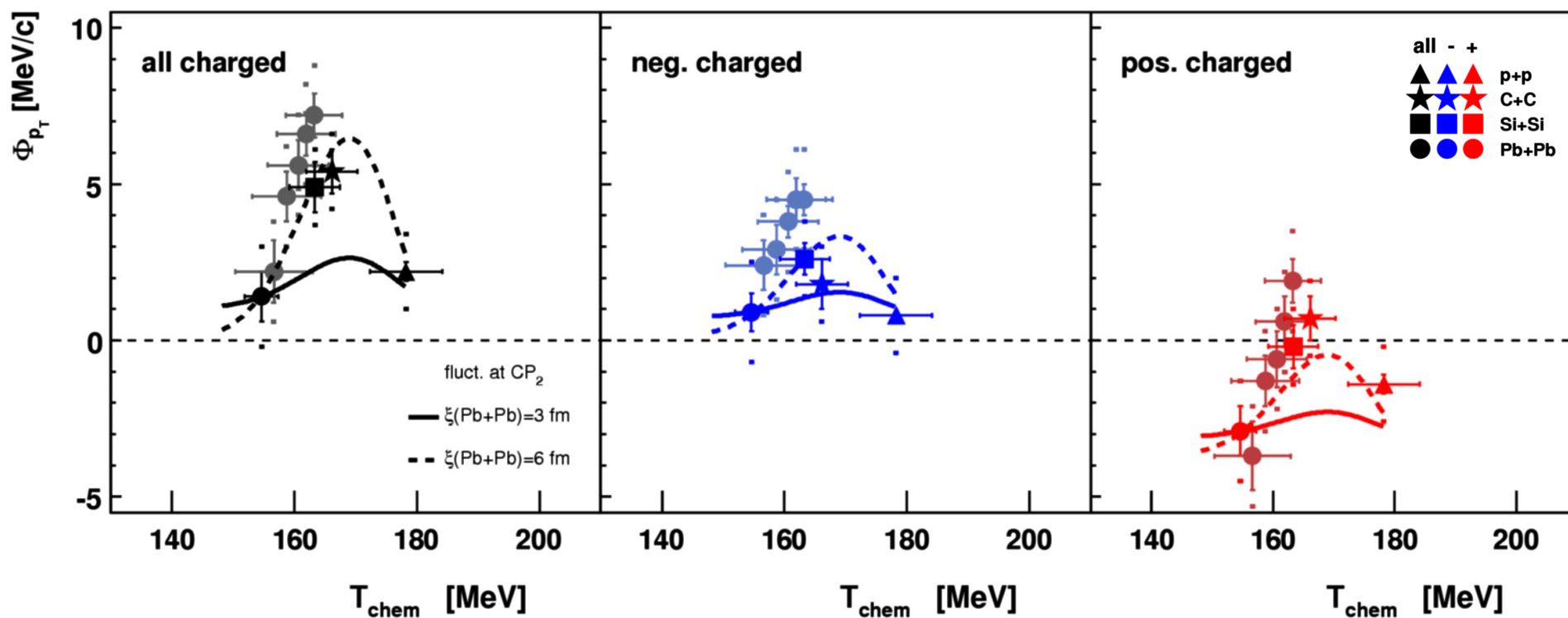
Significant increase of ω for
 peripheral Pb+Pb; a large effect
 can still originate from
 fluctuations of the number of
 target participants

(see V.P. Konchakovski et al., Phys.
 Rev C73, 034902 (2006))



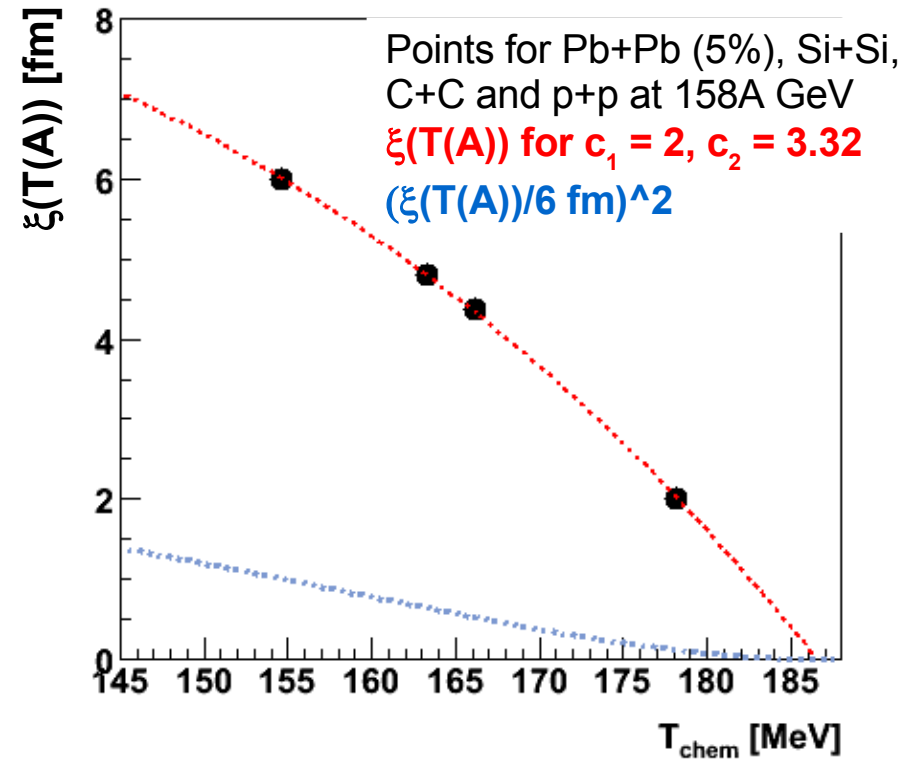
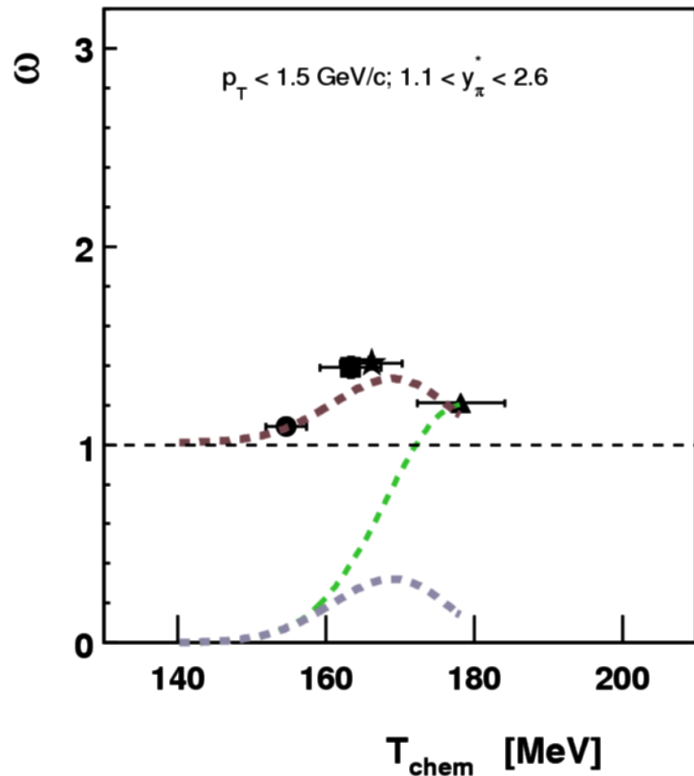
5 remaining centralities of Pb+Pb also shown

NA49 values of T_{chem} for p+p, C+C, Si+Si, and Pb+Pb (5%) - PRC73, 044905 (2006), and for remaining centralities of Pb+Pb (lighter colors) – linear interpolation between two points for Si+Si and Pb+Pb (5%)



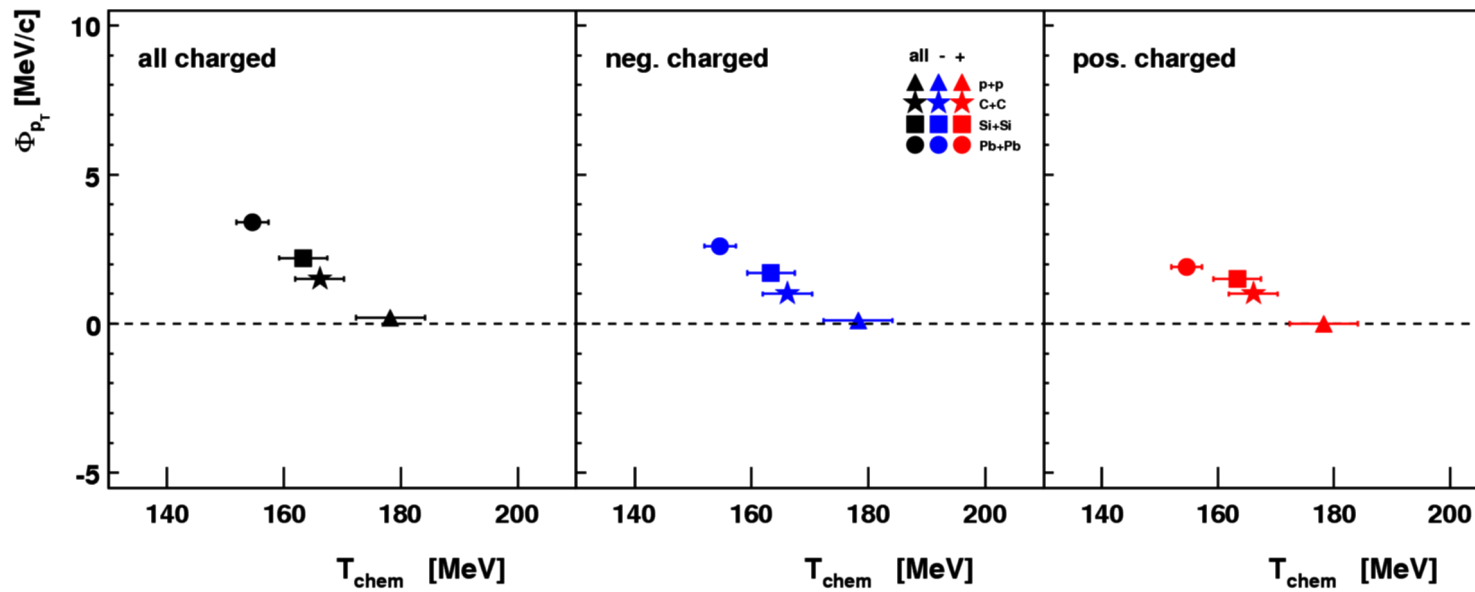
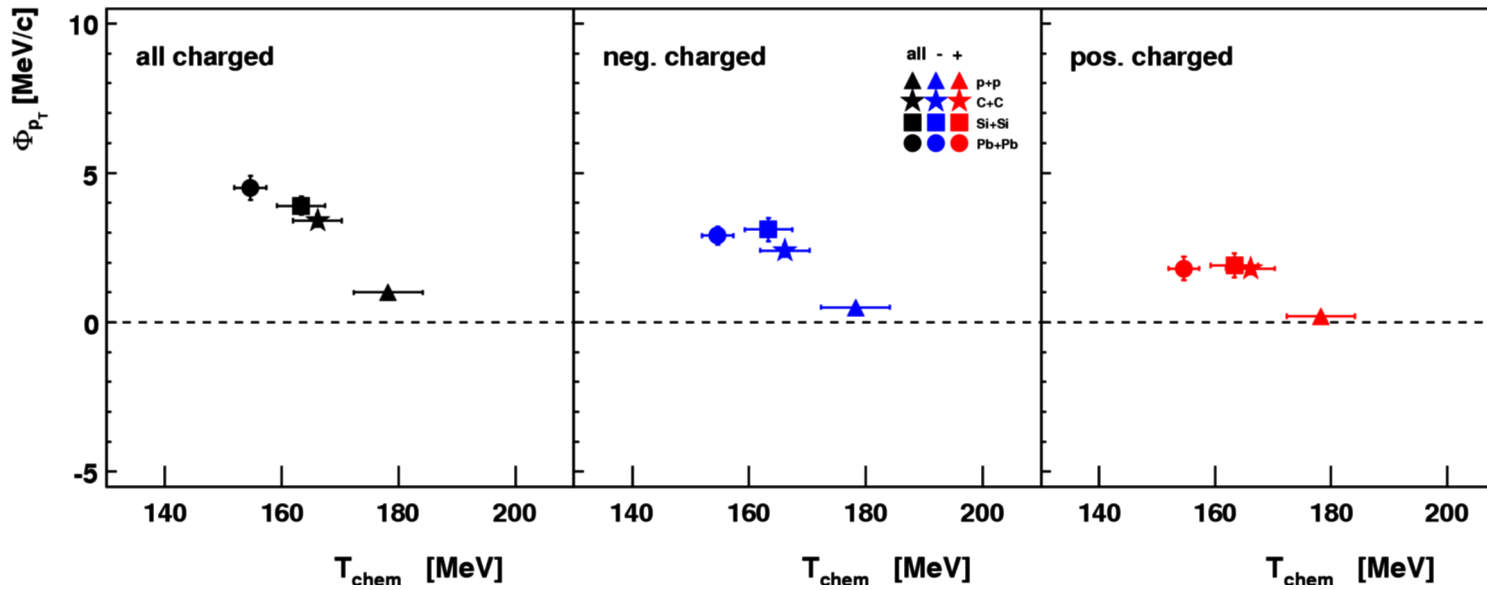
Correlation length $\xi = \min (c_1 A^{1/3}, c_2 A^{1/9})$
 = min (limit due to finite system size, limit due to finite life time)

Assumed correlation length ξ for Pb+Pb = 6 fm
 and for smaller systems ξ decreased



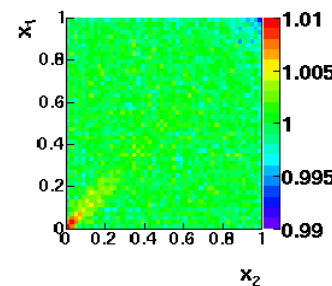
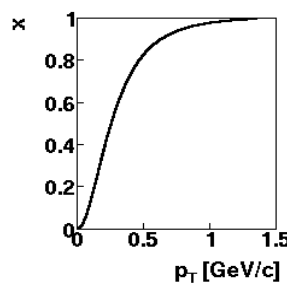
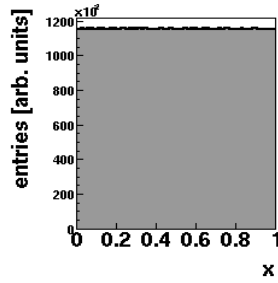
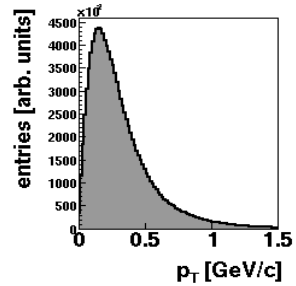
1. Gaussian curve with maximum predicted by M. Stephanov and position at $T_{\text{chem}}(\text{p+p})$
2. multiplied by $(\xi(T(A))/6\text{fm})^2$
3. Finally curve normalized for central Pb+Pb (it is curve shifted to cross Pb+Pb point)

Lower p_T regions



Two-particle correlations in the cumulative variable x

additional information about the source (nature) of dynamical fluctuations



$$x(i) = \int_0^{p_{Ti}} \rho(p_T) dp_T$$

$\rho(p_T)$ - inclusive p_T distribution normalized to unity

$p_T \rightarrow x \rightarrow$ pairs (x_1, x_2) within the same event

Examples:

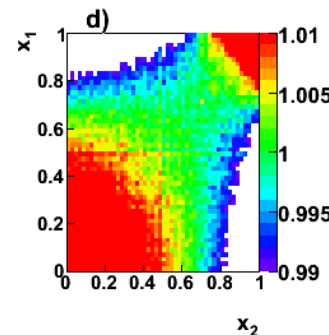
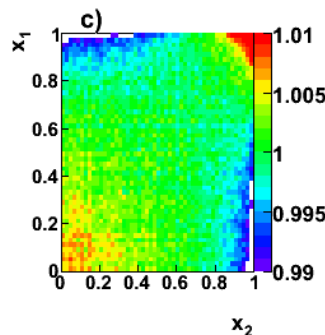
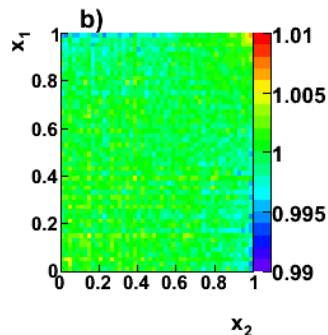
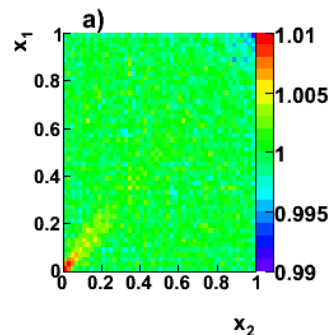
1. Uniform distribution \rightarrow no dynamical fluctuations
2. Structure \rightarrow dynamical fluctuations
 - a) Bose-Einstein and Coulomb correlations – along the diagonal
 - b) E-b-e inverse slope parameter (T) fluctuations – “saddle-shaped” structure

Pb+Pb data

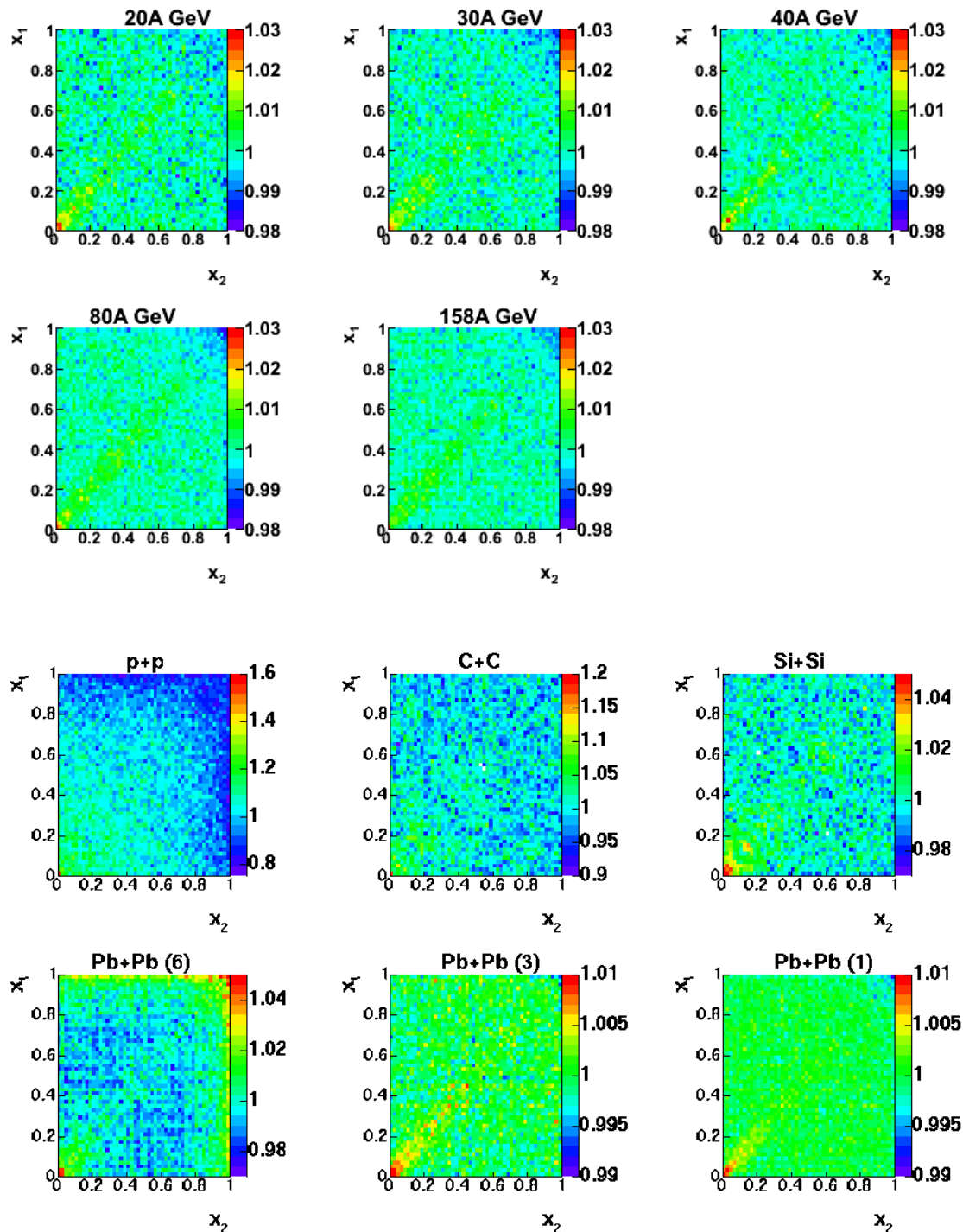
**2.6%, 20 MeV/c
Monte Carlo**

**5.3%, 73 MeV/c
Monte Carlo**

**10.5%, 224 MeV/c
Monte Carlo**



random generator of “ T ” fluctuations for central Pb+Pb interactions at 158A GeV
 T generated from Gauss with σ_T . Given in the panel: σ_T/T [%] and Φ_{PT} [MeV/c]



**Energy dependence
for central Pb+Pb**
(PRC79, 044904 (2009)):
Short range (Bose-
Einstein and Coulomb)
correlations - diagonal

**System size dependence at
158A GeV** (PRC70, 034902, 2004):
For p+p – structure due to $M(p_T)$
vs. N correlation
Pb+Pb: short range (Bose-
Einstein and Coulomb)
correlations - diagonal

$$0.005 < p_T < 1.5 \text{ GeV}/c$$

Elliptic flow of baryons and mesons

- N and p_T fluctuations: CP “memory effects” observed at thermal freeze-out
- Collective flow: shows the possible effect accumulated during the whole evolution, rather than just at the freeze-out
- The energy dependence of anisotropic flow is considered to be sensitive to CP

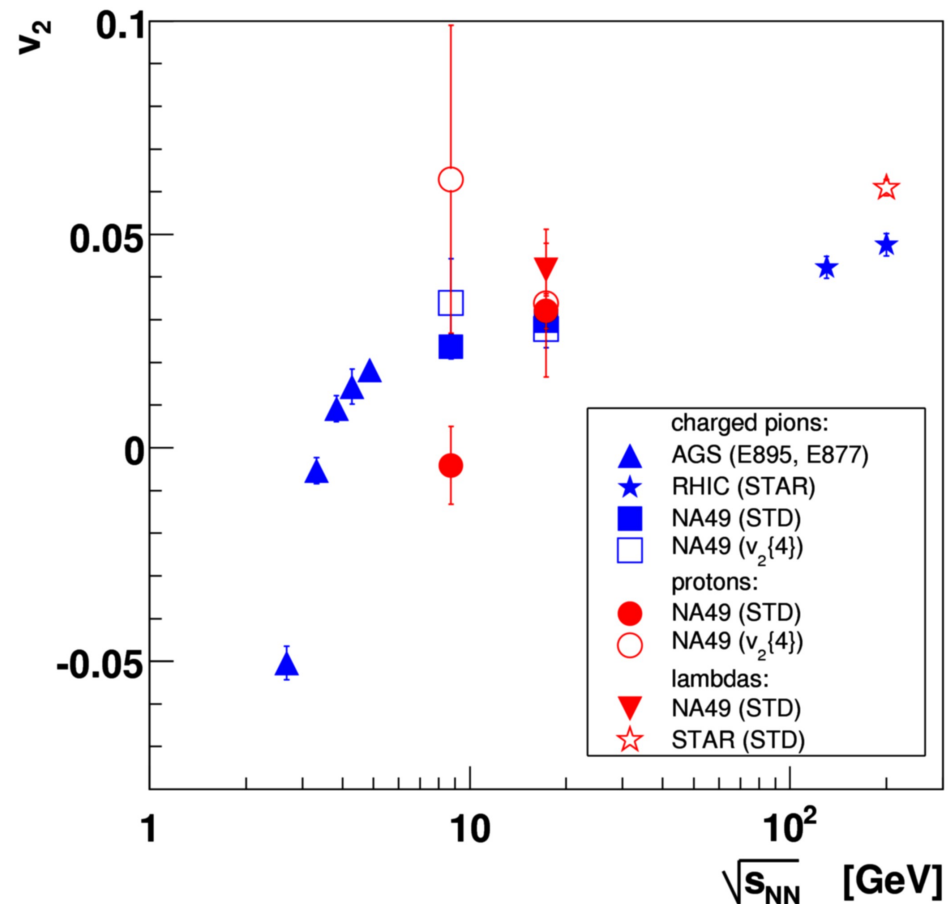
In the presence of CP we expect
(E. Shuryak, arXiv:hep-ph/0504048)

- **decrease of the baryon flow**
- **increase of the meson flow**

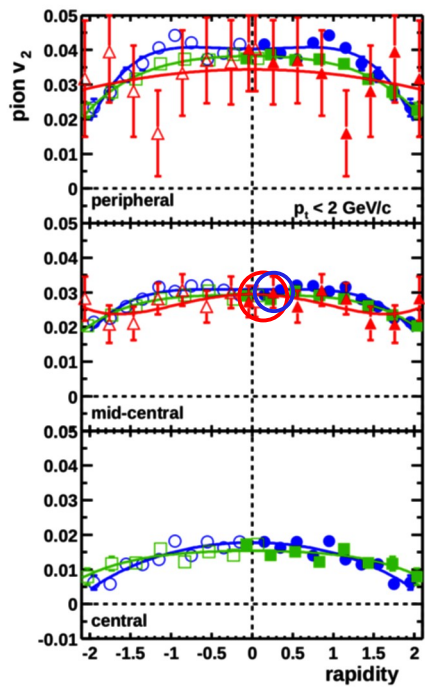
Elliptic flow at mid-rapidity for mid-central
Pb+Pb and Au+Au collisions

NA49: Alt et al., PRC68, 034903 (2003)
Alt et al., PRC75, 044901 (2007)

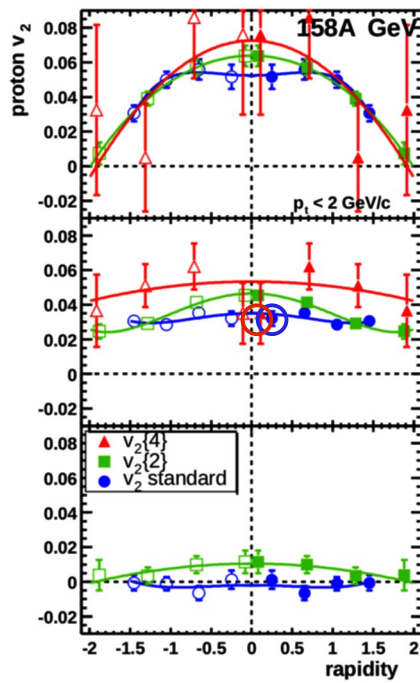
**At SPS energies the energy
dependence of v_2 for baryons is
not established**



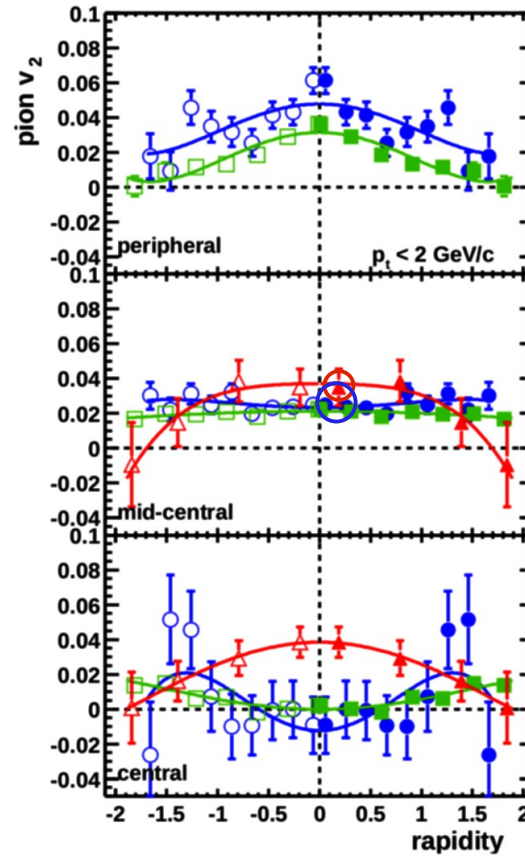
Data are not conclusive; better experiments required for SPS energy range



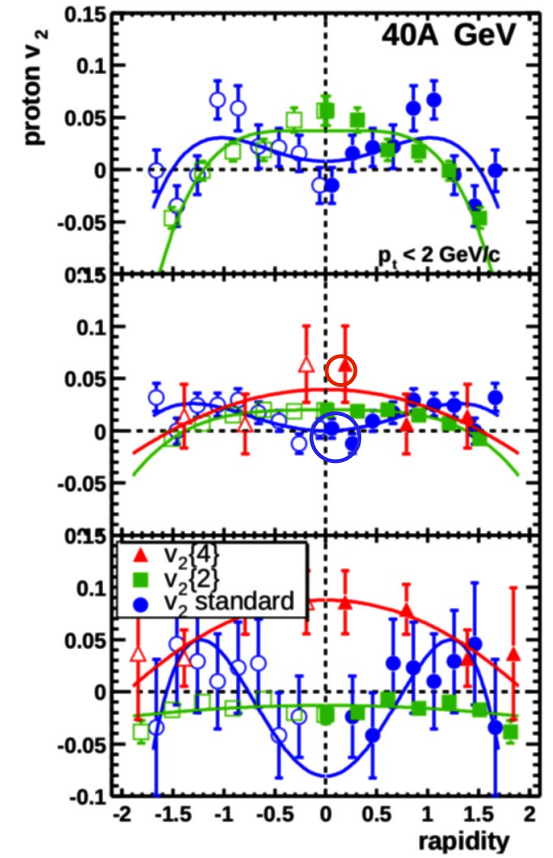
mean values from
two red and two
blue points close to
mid-rapidity



one red and one
blue point close to
mid-rapidity



mean values from
two blue points and
one red point at
mid-rapidity



mean values from
two blue points and
one red point at
mid-rapidity

points shown in excitation
function are at mid-rapidity
 $|y^*| < 0.2-0.3$

C. Alt et al. (NA49 Collab.),
Phys. Rev. **C68**, 034903 (2003)

$$\frac{1}{m_T} \frac{d^2 n}{dm_T dy} = C_1 \exp(-(m_T - m_0)/T_{slope}) + C_2 \exp(-(m_T - m_0)/T')$$

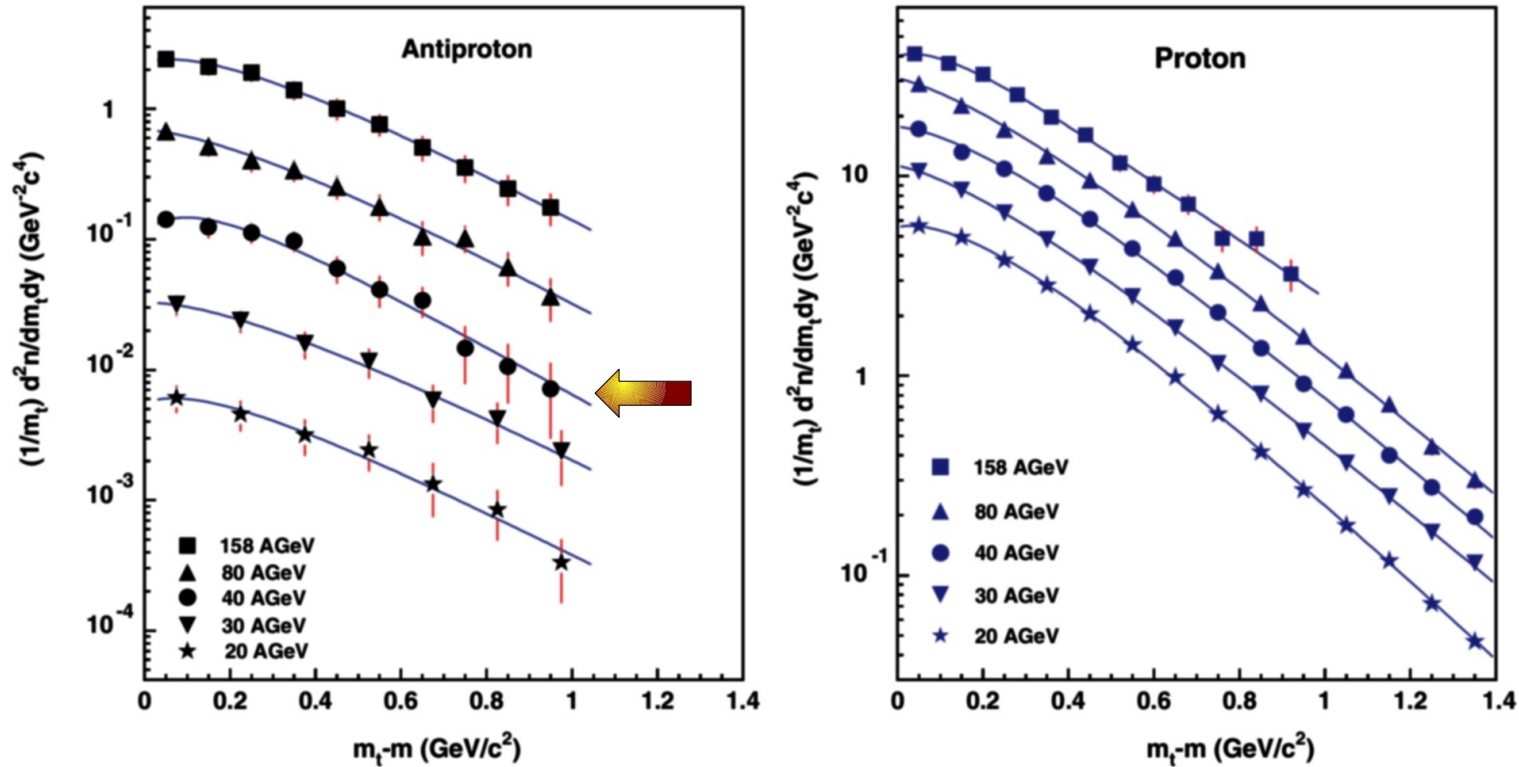
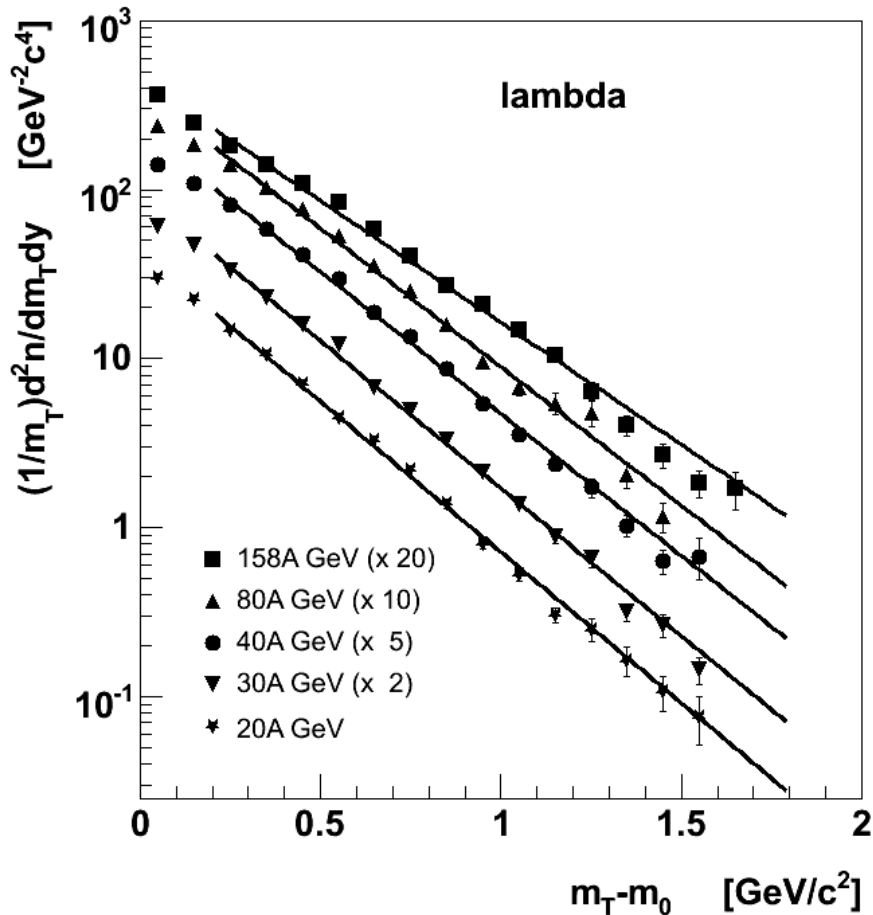


FIG. 3. (Color online) Transverse mass distributions for antiprotons and protons at midrapidity in central Pb+Pb collisions at 20A, 30A, 40A, 80A, and 158A GeV. Errors are statistical. Solid lines illustrate the two-exponential fit of Eq. (1) to the data. For clarity, the spectra are scaled down by a factor of 2 successively from the uppermost data.

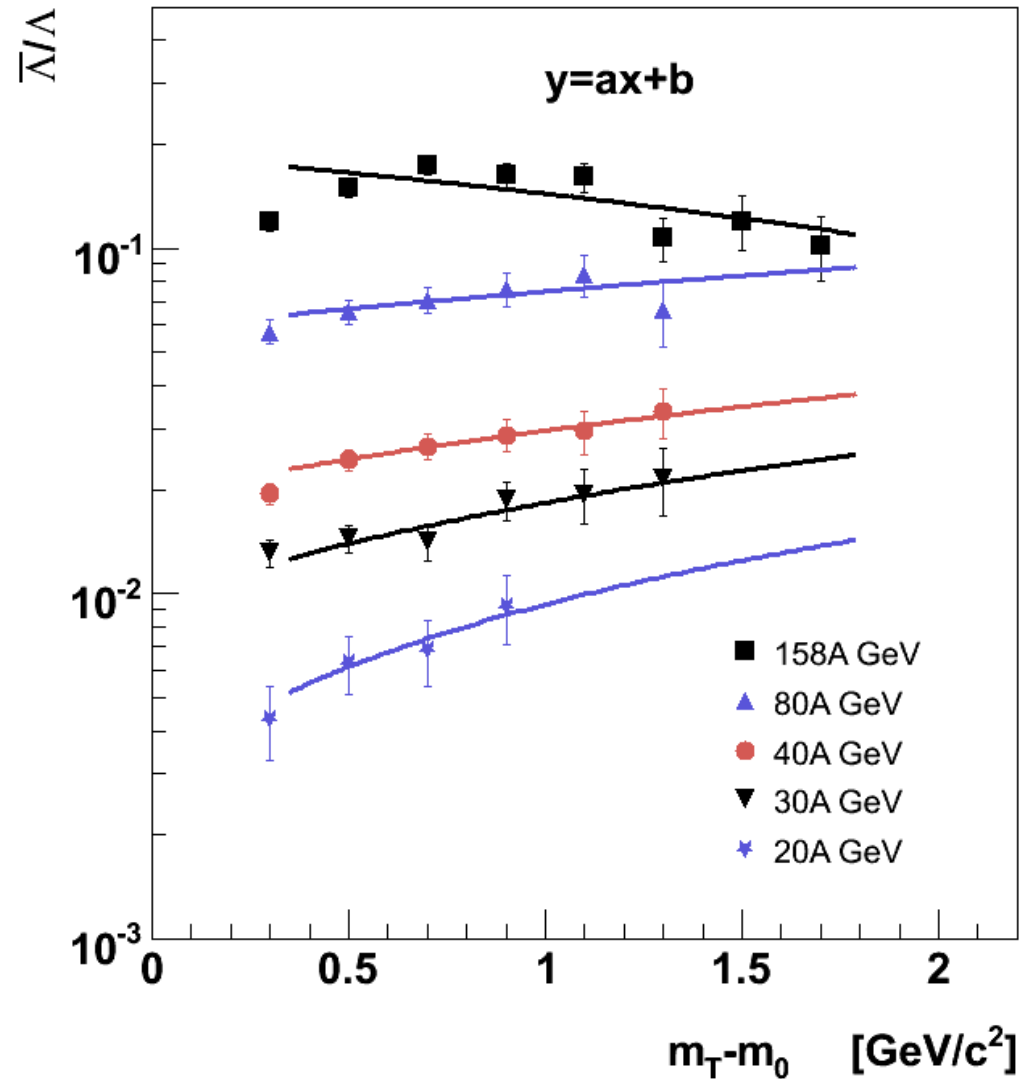
anti-lambda/lambda ratio versus $m_T - m_0$

$$\frac{1}{m_T} \frac{d^2 n}{dm_T dy} \propto \exp\left(\frac{-(m_T - m_0)}{T_{slope}}\right)$$

fit to data in the range $0.2 < m_T - m_0 < 1.8$



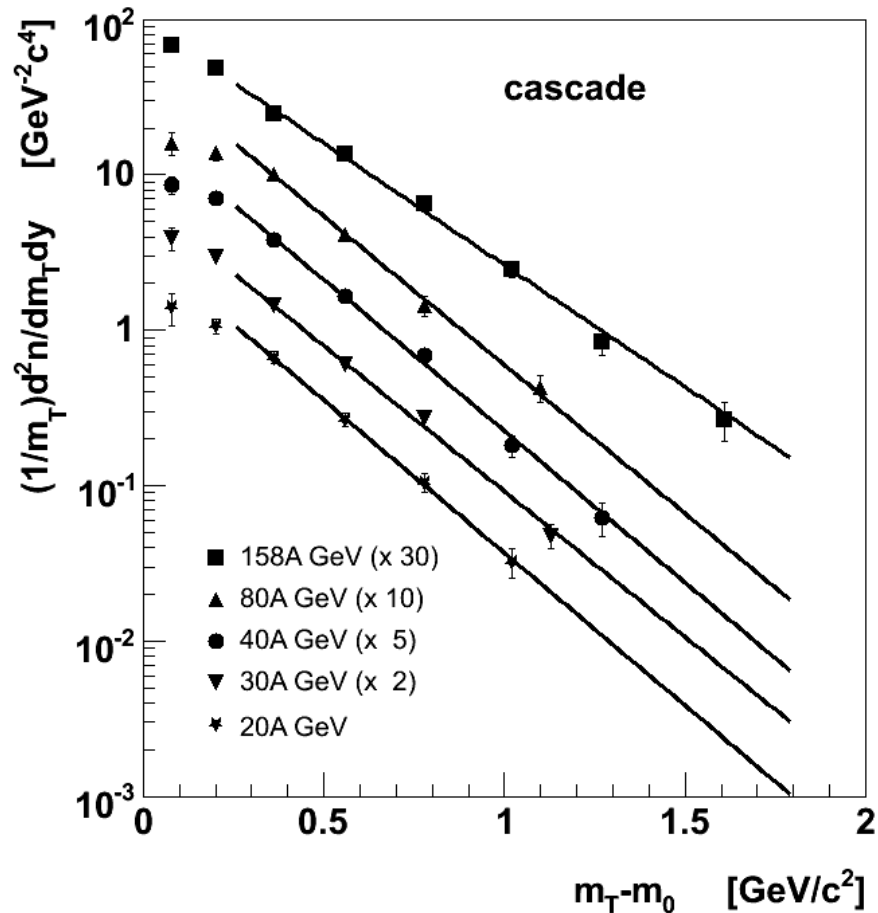
Points for anti-lambdas divided by fitted (left) curves for lambdas



anti-cascades/cascades ratio versus $m_T - m_0$

$$\frac{1}{m_T} \frac{d^2 n}{dm_T dy} \propto \exp\left(\frac{-(m_T - m_0)}{T_{slope}}\right)$$

fit to data in the range $0.25 < m_T - m_0 < 1.8$



Points for anti-cascades divided by fitted (left) curves for cascades

